Diazaborolyl-boryl push-pull systems with ethynylene-arylene bridges as 'turn-on' fluoride sensors.

Lothar Weber*[,a], Daniel Eickhoff[a], Jan Kahlert[a], Lena Böhling[a], Andreas Brockhinke[a], Hans-Georg Stammler[a], Beate Neumann[a] and Mark A. Fox[b]

[a]Fakultät für Chemie der Universität Bielefeld
33615 Bielefeld, Germany
E-Mail: lothar.weber@uni-bielefeld.de
[b]Department of Chemistry, Durham University, South Road, Durham, DH1 3LE, UK.

† Electronic Supplementary Information (ESI) available: Additional photophysical data, Fluoride titration data, TD-DFT data, Additional MO figures and Molecular orbital contributions. See DOI:

Abstract:
Two linear π-conjugated systems with 1,3-diethyl-1,3,2-benzodiazaborolyl [$C_6H_4(NEt_2)_2B$-] as a donor group and dimesitylboryl (-$BMes_2$) as acceptor were synthesised with -ethynylene-phenylene- (-C≡C-1,4-C_6H_4-, **3**) and -ethynylene-thiophene- (-C≡C-2,5-C_4H_2S-, **12**) bridges between the boron atoms. An assembly (**20**) consisting of two diazaborolyl-ethynylene-phenylene-boryl units, [$C_6H_4(NCy)(N')B$-C≡C-1,4-C_6H_4-$BMes_2$] joined via a 1,4-phenylene unit at the nitrogen atoms (N') of the diazaborolyl units was also synthesised. The three push-pull systems, **3**, **12** and **20**, form salts on fluoride addition with the $BMes_2$ groups converted into $(BMes_2F)^-$ anions. The molecular structures of **3**, **12** and **(NBu_4)(12·F)** were elucidated by X-ray diffraction analyses. The borylated systems **3**, **12** and **20** show intense blue luminescence in cyclohexane with quantum yields (Φ_{fl}) of 0.99, 0.44 and 0.94, respectively, but weak blue-green luminescence in tetrahydrofuran (Φ_{fl} = 0.02 - 0.05). The charge transfer nature of these transitions is supported by TD-DFT computations with the CAM-B3LYP functional. Addition of tetrabutylammonium fluoride to tetrahydrofuran solutions of **3** and **20** resulted in strong violet-blue luminescence with emission intensities up to 46 times more than the emission intensities observed prior to fluoride addition. Compounds, **3** and **20**, are demonstrated here as remarkable 'turn-on' fluoride sensors in tetrahydrofuran solutions.

Introduction

Conjugated organic molecules and polymers with three-coordinate boron units as building blocks have attracted considerable interest because of their linear and non-linear optical and electronic properties, which make them potentially useful in functional materials.[1] Three-coordinate boron generally behaves as a π-acceptor due to its vacant p-orbital, which stabilizes the LUMO of an adjacent conjugated π-electron system and thus lowers the HOMO-LUMO gap of these molecules. This field of research has been dominated by the use of the dimesitylboryl group ($BMes_2$, Mes = 2,4,6-$Me_3C_6H_2$), in which the unsaturated boron centre is stabilized towards oxidation and hydrolysis by the steric shielding of the four *ortho*-methyl groups.[2-5] The $BMes_2$ group is considered to have an acceptor strength between that of NO_2- and CN-groups.[6,7] Such electron-deficient compounds are efficient electron-transporting and/or emitting layers in organic light emitting diodes (OLEDs).[5] Compounds with $BMes_2$ groups are often strongly coloured and/or luminescent,[8] which renders them useful as colorimetric or luminescent sensors for fluoride ions.[9-13]

In the past decades, the chemistry of a different class of three-coordinate boron compounds, namely 1,3,2-diazaboroles, has rapidly developed.[14-21] Some of these compounds show strong luminescence when irradiated by UV light. For synthetic reasons the 1,3-diethyl-1,3,2-benzodiazaborole unit is the most frequently employed representative, and compounds containing this group as a substituent are moderately air-stable.[16,22-27] As the $BMes_2$ group is known as an effective acceptor (A) and the benzodiazaborolyl unit has been suggested to be a π-donor (D)[27] the novel "push-pull"-systems [D-bridge-A] with 1,4-phenylene-, 4,4'-biphenylene-, 2,5-thiophene- and 5,5'-dithiophene- scaffolds (**I**-**IV**, Chart I) have been investigated recently.[28] Photophysical studies on these compounds reveal blue-green fluorescence and Stokes shifts for the first three representatives of 7820-9760 cm^{-1} in THF, whereas the Stokes shift for the last compound is significantly smaller (5510 cm^{-1} in THF).

Thereby the π-donating strength of the 1,3-diethyl-1,3,2-benzodiazaborolyl substituent was found to lie between that of the MeO- and the Me_2N- groups. It is well documented that the absorption- as well as the emission-bands of a boron functionalized conjugated π-system can be shifted to lower energies by elongation of the latter.[29]

The 2-arylethynyl-1,3,2-benzodiazaboroles, **V**-**X** (Chart I), were shown to be highly luminescent with quantum yields (Φ_{fl}) of 1.00 and 0.96 in cyclohexane and THF, respectively for **V**. [27] Thus, it was logical to insert an acetylenic unit between the benzodiazaborolyl group and the adjacent arene- or heteroarene-ring in the push-pull systems of **I** and **III** respectively. Here the syntheses, characterisation and photophysics of these compounds and of two assemblies, where two linear 2-aryl-1,3,2-benzodiazaborole units are linked via a phenylene unit, are described. The intriguing fluoride-sensing properties of the push-pull systems are also explored as such molecules have potential use as luminescent sensors for anions such as fluoride.

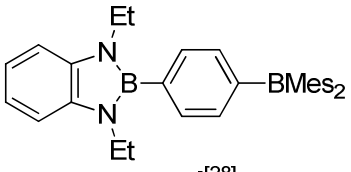

I[28]

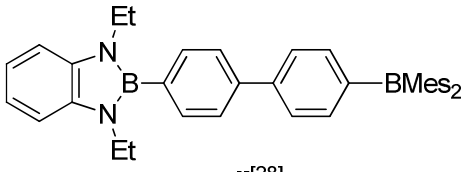

II[28]

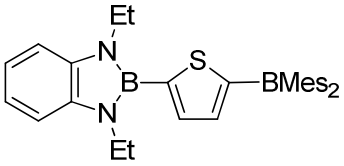

III[28]

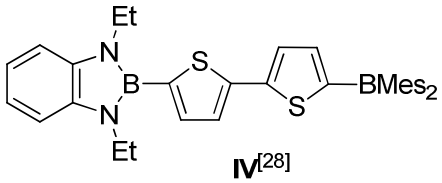

IV[28]

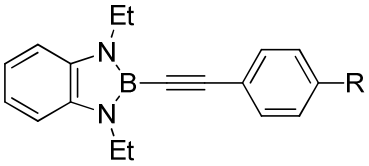

R = H(**V**), Me(**VI**), OMe(**VII**), SMe(**VIII**), NMe_2(**IX**), Br(**X**)[25-27]

Chart I

Results and discussion

The reaction of *in situ* lithiated 4-dimesitylboryl-phenylacetylene **2**[30] with an equimolar amount of 2-bromo-1,3-diethyl-1,3,2-benzodiazaborole **1**[16] in *n*-hexane at room temperature led to the formation of diazaborolylated 4-dimesitylboryl-phenylacetylene **3** as colourless platelets in 90% yield (Scheme 1). The combination of equimolar amounts of **3** with tetrabutylammonium fluoride (TBAF) resulted in the formation of the salt [n**Bu$_4$N**][**3·F**].

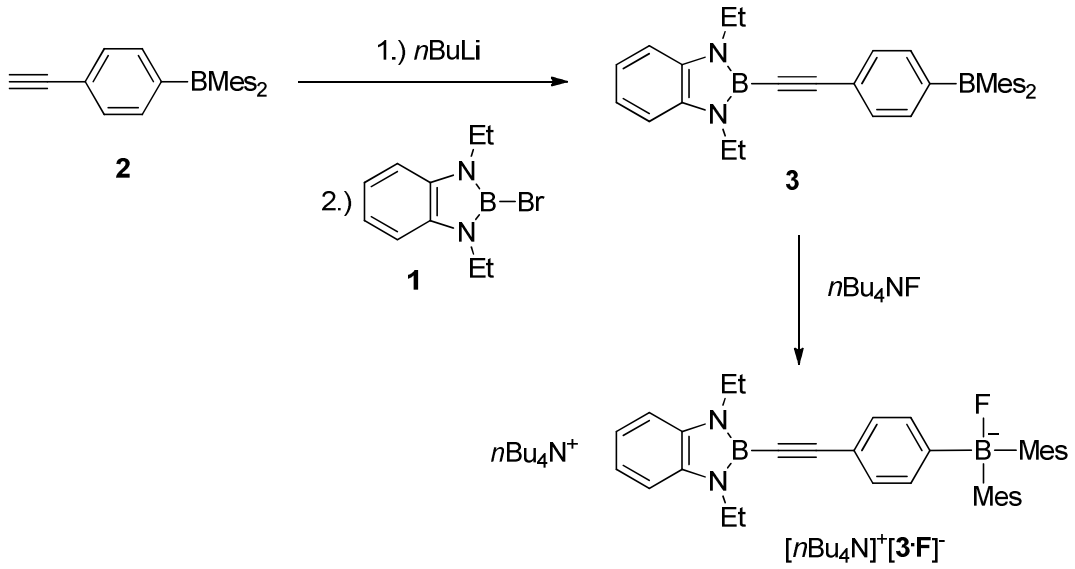

Scheme **1**. Syntheses of **3** and $[n\text{Bu}_4\text{N}]^+[\mathbf{3{\cdot}F}]^-$.

For comparison with closely related derivatives **3** and **V**-**X**, the cyano compound **5** was synthesized here by the lithiation of 4-cyanophenylacetylene **4**[31] in THF and the subsequent treatment of the organolithium species with an equimolar amount of 2-bromo-1,3,2-benzodiazaborole **1**. The lithiating reagent, $\text{LiN(SiMe}_3)_2$ was used here as *n*BuLi reacts with the CN group of **4**. Diazaborole **5** was isolated as colourless needles in 69% yield (Scheme 2).

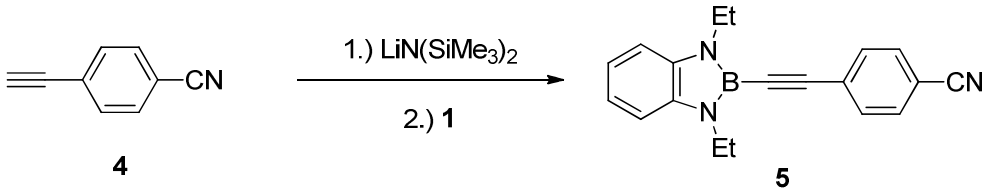

Scheme **2**. Synthesis of **5**.

Compound **12**, where the benzodiazaborolyl- and dimesitylboryl- units are separated by a 2,5-thiophene-diyl bridge was synthesised from 2-(trimethylsilylethynyl) thiophene **8**[32] by treatment with an equimolar amount of *n*-butyllithium in diethyl ether at room temperature and the subsequent addition of an ethereal solution of dimesityl fluoroborane (**9**).[33] After the addition of brine to the reaction mixture crude 2-(silylethynyl)-5-dimesitylboryl-thiophene was isolated in ca. 95% yield. Complete characterization of intermediate **10** was disclaimed in favour of its subsequent desilylation by means of potassium carbonate in a mixture of dichloromethane and methanol to afford 2-(ethynyl)-5-dimesitylboryl-thiophene (**11**) in 62% yield. The synthesis of target compound **12** was accomplished by lithiation of **11** and coupling with 2-bromo-1,3,2-benzodiazaborole in *n*-hexane, and **12** was obtained as large colourless crystals in 54% yield. Compound **12** was converted into its crystalline fluoride adduct $[n\text{Bu}_4\text{N}]^+\mathbf{[12{\cdot}F]}^-$ by addition of 1 equiv. of $\text{TBAF}{\cdot}3\text{H}_2\text{O}$ in C_6D_6 (Scheme 3).

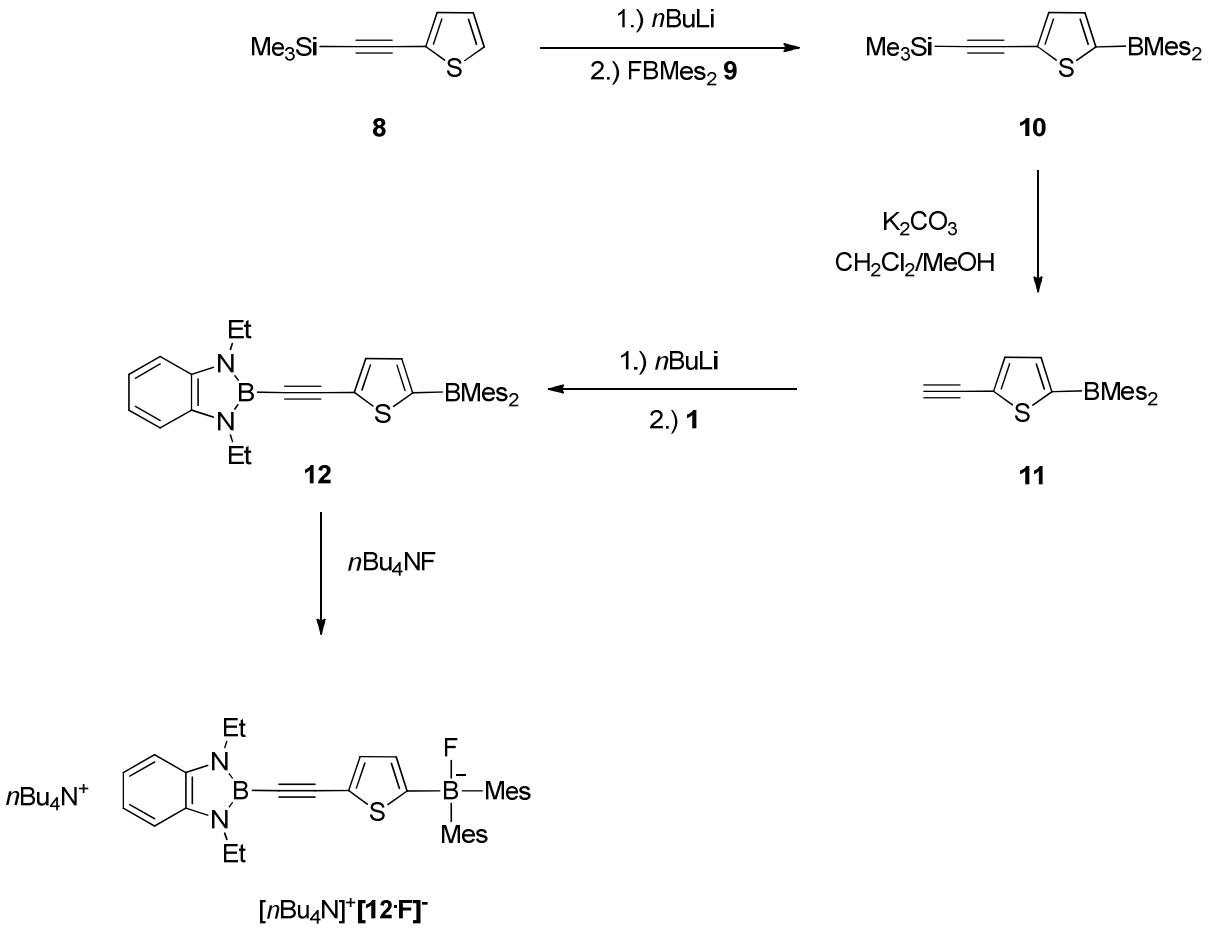

Scheme **3**. Syntheses of **12** and $[n\text{Bu}_4\text{N}]^+[\mathbf{12{\cdot}F}]^-$.

The compound 2-isopropylamino-1-bromobenzene **13**, was used for the synthesis of a bisborole with two diazaborole molecules (like **V** and **3**) linked by a spacer. The synthesis of the precursor triphenylene-tetraamine **14** was accomplished by a Hartwig-Buchwald coupling between *p*-phenylenediamine and two equiv. of 2-isopropylamino-1-bromobenzene **13** in boiling toluene utilizing an *in situ* prepared catalyst (prepared from 1,3-bis-2´,6´-diisopropylphenyl)imidazolium chloride (IPr·HCl), sodium *tert*-butanolate and $Pd(OAc)_2$ in toluene) (Scheme **4**), (71% yield).[34] Treatment of **14** with 2 equiv. of boron tribromide in the presence of an excess of calcium hydride in CH_2Cl_2 afforded the 1,4-bis(2'-bromo-1',3',2'-benzodiazaborol-1-yl)1'-benzene derivative **15** as colourless crystals in 62% yield. Combination of the bis(bromoborole) **15** with 2 equiv. of *in situ* generated lithium phenylacetylide in *n*-hexane furnished the bis-benzodiazaborole **16** as a microcrystalline solid in 53% yield after crystallisation from an *n*-hexane/CH_2Cl_2 mixture.

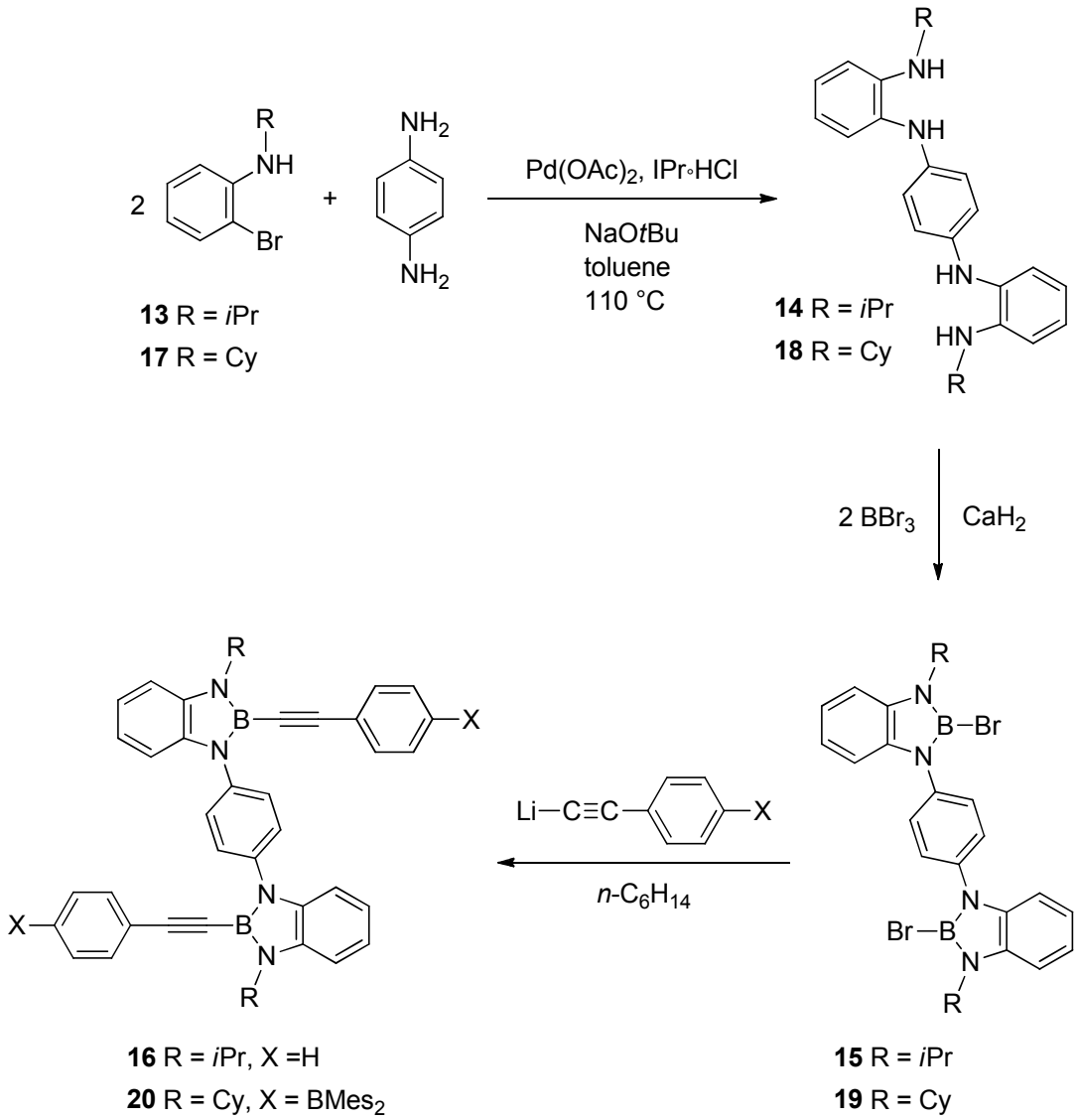

Scheme **4**. Syntheses of **16** and **20**.

Whereas the product from **15** with lithiated 4-dimesitylboryl-phenylacetylene[30] could not be isolated as a pure compound, the cyclohexyl bromoaniline **17** was successfully used to obtain a soluble bisborole **20** with two $BMes_2$ groups. Triphenylene tetraamine **18** was synthesised analogously from 2 equiv. of bromoaniline **17** and 1,4-phenylenediamine as colourless crystals in 51% yield. Two-fold cyclocondensation with 2 equiv. of BBr_3 led to the bis(bromodiazaborolyl)benzene derivative **19** (43% yield). The synthesis of target molecule **20** was completed by reaction of 2 equiv. of lithiated 4-dimesitylboryl-phenylacetylene[30] and **19** in toluene. Product **20** was isolated from the reaction residue as a microcrystalline colourless solid by continuous extraction with *n*-hexane over a period of two weeks.

Compounds **3**, **5**, **12**, **16** and **20** are stable to oxygen and moisture, whereas the bromo derivatives **15** and **19** decompose in air. The new compounds are well soluble in benzene, toluene, dichloromethane and chloroform and only poorly soluble in alkanes. The $^{11}B\{^1H\}$ NMR spectra of all new compounds **3**, **5**, **12**, **15**, **16**, **19** and **20** display singlets in the narrow range of 20.2-23.5 ppm for the boron nuclei of the benzodiazaborole units. Singlet resonances at 74.4-74.9 ppm were observed for the dimesitylboryl groups at phenylene units, whereas the

corresponding singlets seen in the thiophene derivatives, **10**-**12**, were significantly shielded (65.2-66.8 ppm). Singlet resonances at δ = 21.4 and 5.0 ppm were registered for the benzodiazaborole part and the $BMes_2F$ unit, respectively, for the anions [**3·F**]$^-$ and [**12·F**]$^-$.

X-ray Crystallography

Molecular structures were determined for the two benzodiazaborolyl-functionalized dimesitylboryl(hetero)arylacetylenes **3**, **12**, [nBu$_4$N]$^+$**[12·F]**$^-$ and the 1,4-bis(benzodiazaborol-5-yl)benzene **15** (Figures 1-3). Bond lengths and angles of interest are listed in Table 1.

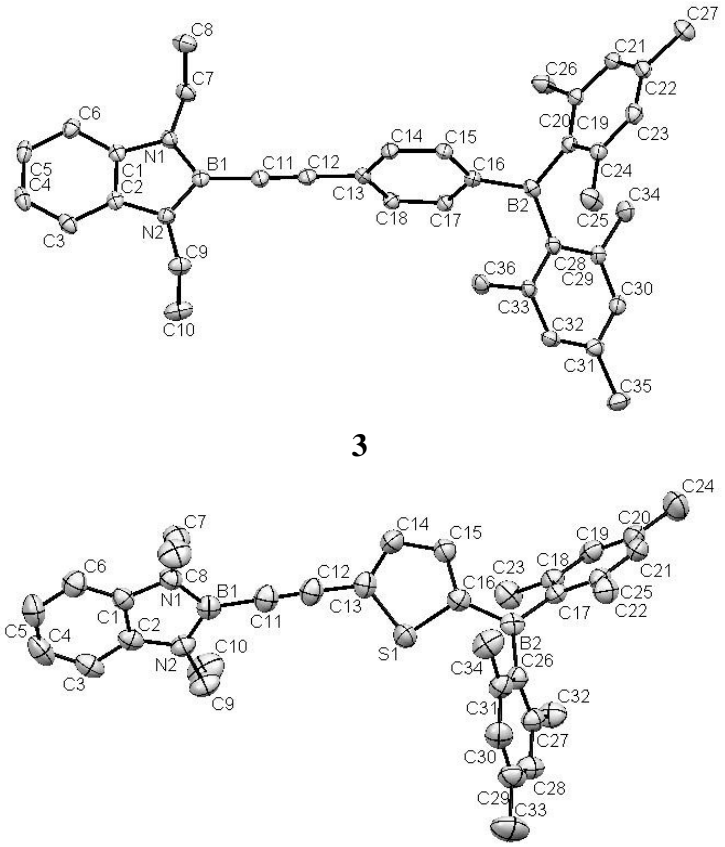

3

12

Figure **1**. Molecular structures of **3** and **12**. Hydrogen atoms are omitted for clarity.

Molecule **3** is constructed from a benzodiazaborole ring that is linked to the arylalkynyl unit by a B(1)-C(11) single bond of 1.528(3) Å, which compares well with the corresponding bond length in **V** (1.524(2) Å). The length of the triple bond C(11)-C(12) is 1.205(3) Å. Valence angles at the nearly linear bridge between the two rings B(1)-C(11)-C(12) and C(11)-C(12)-C(13) are 177.8(2)° and 178.8(2)°. The planes between the central benzene ring and the heterocycle are twisted by 88.2°. The benzene ring is attached in the 4-position to the dimesitylboryl group by a B(2)-C(16) single bond [1.565(3) Å]. B-C bonds at the mesityl groups in **3** are in the expected range [B(2)-C(19) 1.581(3), B(2)-C(28) 1.578(3) Å]. The plane defined by the C(16), C(19) and C(28) atoms, including the boron atom, is twisted out

of the plane of the benzene ring by 42.2°. The interplanar angles between this plane and the mesityl groups are 52.9° and 57.7°. Bond lengths and bond angles within the benzodiazaborole part of **3** are similar to those of numerous diazaboroles studied before.[17, 19, 22, 25-27]

The molecule **12** may be described as a benzodiazaborole which is connected with a 2-thienylethynyl unit via the B(1)-C(11) single bond of 1.520(3) Å. Both heterocycles are linked by an essentially linear ethynyl bridge with a triple bond C(11)-C(12) bonds of 1.207(3) Å and angles B(1)-C(11)-C(12) and C(11)-C(12)-C(13) of 176.4(2)° and 178.2(3)°, respectively. The planes of the heterocycles enclose a dihedral angle of 44.9°, which has about half the size than the corresponding angle in **3**. The 5-position of the thiophene ring is substituted by a dimesitylboryl unit via a B(2)-C(16) single bond of 1.541(3) Å. As given in **3** the mesityl relevant B-C bonds B(2)-C(17) [1.579(3) Å] and B(2)-C(26) [1.578(3) Å] are as expected. The plane defined by the atoms C(16), C(17) and C(26), including atom B(2), is twisted out of the thiophene plane by 20.4°. The interplanar angles between this plane and the mesityl groups are 58.0° and 60.2°.

Crystals of the adduct $[n\mathrm{Bu_4N}]^+$**[12·F]**$^-$ contain 4 pairs of independent molecules (**A**-**D**) in the unit cell (Fig. 2; Table 1). Bond lengths and bond angles were essentially identical within 3esds. Significant deviations were found for the angle C-C-C at the acetylene bridge which for molecule **B** is more bent (176.8(3)°) than for the three other molecules (178.1(3)-178.7(3)°). The angle B-C-C varies from 169.2(2)° in **D** *via* 173.5(2)° in **A**, 175.0(2)° in **B** to 176.8(3)° in **C**. The interplanar angles between the heterocycles vary in the series 40.4° (**B**) < 43.8° (**D**) < 46.8° (**C**) < 52.4 (**A**), which are not significantly different as the respective angle in **12** (44.9°). The geometric parameters within the Mes_2BF-unit (Table 1) are comparable to those in other triaryl fluoroborates.[9a, 10e] No other significant changes in the structural parameters of the BDB−C≡C−C_4H_2S− part of **12** upon fluoride addition were observed.

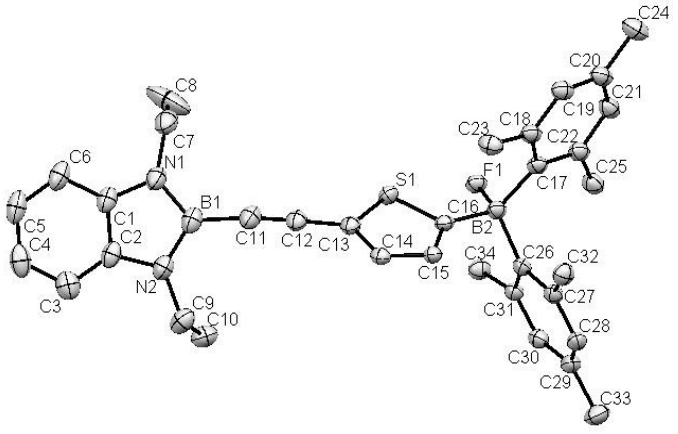

[12·F]$^-$

Figure 2. Structure of one independent molecule (**A**) (out of four) in the unit cell of the anion **[12·F]**$^-$ in $[Bu_4N]$[**12·F**]. Hydrogen atoms are omitted for clarity.

Compound **15** may be described as a benzene ring that is substituted at the *para*-positions by two 2-bromo-3-isopropyl-1,3,2-benzodiazaborol-1-yl units via N(1)-C(10) single bonds of 1.427(4) Å. (Figure 3) The molecule possesses a centre of inversion in the middle of the benzene spacer. The planes of benzodiazaborole rings and the benzene unit enclose dihedral angles of 51.7°. Bond lengths and angles within the benzodiazaborole part of **15** are comparable to **3** and other benzodiazaboroles.[19, 21-23, 25-28] In summary, molecule **15** is closer to planarity than the $BMes_2$-analogue **3**.

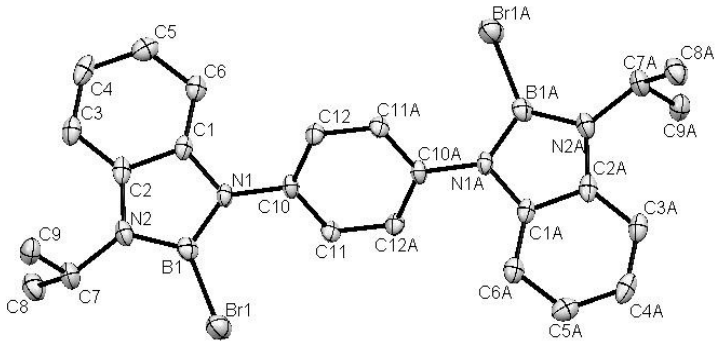

15

Figure 3. Molecular structure of the bisborole **15**. Hydrogen atoms are omitted for clarity.

Table 1. Selected bond lengths and angles for **3**, **12**, **[12·F]**$^-$ and **15**.

	3	**12**	**[12·F]**$^-$ [a]	**15**
Bond lengths (Å)				
B–N	B(1)-N(1) 1.425(3) B(1)-N(2) 1.427(3)	B(1)-N(1) 1.425(3) B(1)-N(2) 1.422(3)	B(1)-N(1) 1.422(3) B(1)-N(2) 1.427(3)	B(1)-N(1) 1.433(5) B(1)-N(2) 1.411(5)
B–C	B(1)-C(11) 1.528(3) B(2)-C(16) 1.565(3) B(2)-C(19) 1.581(3) B(2)-C(28) 1.578(3)	B(1)-C(11) 1.520(3), B(2)-C(16) 1.541(3) B(2)-C(17) 1.579(3) B(2)-C(26) 1.578(3)	B(1)-C(11) 1.533(3) B(2)-C(16) 1.646(3) B(2)-C(17) 1.667(3) B(2)-C(26) 1.648(3)	
B–Hal			B(2)-F(1) 1.477(2)	B(1)-Br(1) 1.925(5)
C–C	C(11)-C(12) 1.205(3) C(12)-C(13) 1.437(2) C(13)-C(14) 1.398(3) C(14)-C(15) 1.390(3) C(15)-C(16) 1.403(3) C(16)-C(17) 1.401(3) C(17)-C(18) 1.381(3) C(13)-C(18) 1.402(3)	C(11)-C(12) 1.207(3) C(12)-C(13) 1.425(3) C(13)-C(14) 1.371(3) C(14)-C(15) 1.404(3) C(15)-C(16) 1.375(3)	C(11)-C(12) 1.211(3) C(12)-C(13) 1.422(3) C(13)-C(14) 1.378(3) C(14)-C(15) 1.411(3) C(15)-C(16) 1.383(3)	C(10)-C(11) 1.389(5) C(11)-C(12A) 1.389(5) C(10)-C(12) 1.389(5)
C–N	N(1)-C(1) 1.395(2) N(2)-C(2) 1.401(2) N(1)-C(7) 1.455(2) N(2)-C(9) 1.463(2)	N(1)-C(1) 1.392(2) N(2)-C(2) 1.391(2) N(1)-C(7) 1.460(3) N(2)-C(9) 1.462(3)	N(1)-C(1) 1.396(3) N(2)-C(2) 1.396(3) N(1)-C(7) 1.463(3) N(2)-C(9) 1.459(3)	N(1)-C(1) 1.401(5) N(2)-C(2) 1.401(5) N(2)-C(7) 1.477(5) N(1)-C(10) 1.427(4)
C–S		S(1)-C(13) 1.711(2) S(1)-C(16) 1.722(2)	S(1)-C(13) 1.734(2) S(1)-C(16) 1.732(2)	
Bond Angles (°)				
C–C–C	C(11)-C(12)-C(13) 178.8(2)	C(11)-C(12)-C(13) 178.2(3)	C(11)-C(12)-C(13) 178.7(2) [176.3(2); 178.1(2); 178.7(2)]	
B–C–C	B(1)-C(11)-C(12) 177.8(2)	B(1)-C(11)-C(12) 176.4(2)	B(1)-C(11)-C(12) 173.5(2) [175.0(2); 176.8(2); 169.2(2)]	
Torsion Angles (°)				
	N(1)-B(1)…C(13)-C(14) 89.6 C(19)-B(2)-C(16)-C(15) 42.5 C(28)-B(2)-C(16)-C(17) 37.0	N(1)-B(1)…C(13)-C(14) 44.9 C(15)-C(16)-B(2)-C(26) 21.2 C(15)-C(16)-B(2)-C(17) 160.4	N(2)-B(1)…C(13)-C(14) 48.0 [42.1; 48.7; 38.8] C(17)-B(2)-C(16)-C(15) 83.8 [81.4; 85.2; 85.3] C(26)-B(2)-C(16)-C(15) 48.7 [49.1; 42.9; 47.7] F(1)-B(2)-C(16)-C(15) 165.2 [166.6; 161.6; 163,6] F(1)-B(2)-C(16)-S(1) 9.2 [14.6; 18.4; 11.4]	C(1)-N(1)-C(10)-C(12) 49.5

[a] Bond lengths and bond angles shown here are from molecule **A**.

Photophysics

Neutral Species

Photophysical measurements for the new compounds **3**, **5**, **12**, **16** and **20** in cyclohexane and THF solutions are summarised in Table 2. For comparison, the reported absorption and emission data for related systems **I**-**V** (Chart I) in cyclohexane and THF solutions are included.[27,28] Photophysical data for compounds **3**, **12** and **20** in other solvents (toluene, chloroform, dichloromethane, acetonitrile) are listed in Table S1 and shown in Figures S1 and S2.

The absorption maxima of **3** and **5** are shifted to lower energies with respect to the closely related analogues, **V-X** (Chart I)**,** showing that such π-acceptors, CN and $BMes_2$, lower the HOMO-LUMO energy gaps. The absorption spectra of the bisdiazaborole **16** in cyclohexane and THF show absorption maxima that are identical to the parent monodiazaborole, **V**, but the extinction coefficients are at least twice as large for **16** compared to **V**. The absorption bands of compound **20** are comparable to that of the closely related monodiazaborole **3**. The extinction coefficients in cyclohexane are similar for both compounds but the extinction coefficient in THF is doubled for **20** compared to **3**. The larger extinction coefficients observed for the bisdiazaboroles compared to the closely related monodiazaboroles are simply due to twice as many chromophores present in a solution of similar molarity when comparing the linked species with the 'monomeric' ones.

All the neutral diazaboroles listed in Table 2 exhibit intense blue/green luminescence under UV-irradiation in cyclohexane solutions with high quantum yields of 0.94-0.99 for three compounds, **3**, **16** and **20**, containing the phenylene-acetylene moieties. Compound **16** also has a high quantum yield Φ_{fl} of 0.82 in THF but the $BMes_2$ systems **3** and **20** have very low Φ_{fl} values of 0.02-0.03 in THF. These quantum yields mirror those found for the related systems, the unsubstituted derivative **V** and the $BMes_2$ derivatives **I** and **II** respectively. The Stokes shifts observed in the regions of 4000-7000 cm^{-1} in cyclohexane and 7000-10000 cm^{-1} in THF are typically found in related benzodiazaboroles reported elsewhere.[19p,27,28]

Small positive solvatochromic shifts were observed in the absorption spectra recorded in cyclohexane, THF, dichloromethane, chloroform and toluene solutions (Tables 2 and S1). However, a negative solvatochromic effect of 300 cm^{-1} was found for nitrile **5** in THF and implies that the ground-state geometry for **5** is relatively polar (and thus more stable in polar solvents) compared to the other diazaboroles observed here. Negative solvatochromic shifts between 600 and 1500 cm^{-1} were observed in the absorption spectra for **3**, **12** and **20** recorded in acetonitrile, a solvent with a high dielectric constant, with the largest negative shift found for compound **12** (Table S1).

Table 2. Photophysical data for **3**, **5**, **12**, **16**, **20** and related compounds, **I-V**.

	In cyclohexane solution					In THF solution					Solvatochromic shifts	
	$\lambda_{max,\ abs}$ [nm]	ε [$Lmol^{-1}cm^{-1}$]	$\lambda_{max,\ em}$ [nm]	Stokes shift [cm^{-1}]	Φ_{fl}	$\lambda_{max,\ abs}$ [nm]	ε [$Lmol^{-1}cm^{-1}$]	$\lambda_{max,\ em}$ [nm]	Stokes shift [cm^{-1}]	Φ_{fl}	absorption [cm^{-1}]	emission [cm^{-1}]
3	342	21300	421	5400	0.99	342	18100	503	9300	0.02	0	3900
5	343	7400	411	4900	0.22	339	12000	477	8500	0.05	-300	3300
12	372	22500	441	4200	0.44	374	24900	516	7300	0.05	200	3300
16	307	44300	379	6600	0.96	307	32700	399	7700	0.82	0	1100
20	344	22200	429	5800	0.94	343	38200	495	9000	0.03	-100	3100
I	327	29600	408	6000	0.99	329	31600	477	9400	0.08	200	3400
II	328	23900	399	5400	0.99	331	25900	489	9800	0.02	300	4300
III	345	19400	439	6200	0.81	350	20100	482	7900	0.46	400	1600
IV	389	11400	430	2500	0.85	392	32800	500	5500	0.45	200	3100
V	307	10400	345	3600	1.00	307	18300	394	7200	0.96	0	3600

Large solvatochromic effects between 3000 and 4000 cm^{-1} were observed from the emission maxima on going from cyclohexane to THF in most diazaboroles. One exception is compound **16** which has a shift value of only 1100 cm^{-1} and may adopt a less polar excited state than other compounds listed in Table 2. The solvatochromic shifts also correspond to solvent polarities in other solvents except for acetonitrile (Table S1). Two emission bands were observed in acetonitrile for **3** (394 and 550 nm), **12** (391 and 567 nm) and **20** (410 and 546 nm) with the longer wavelength expected from the highly polar solvent (Figure 4). Similar bands have been reported for other push-pull systems with -$BMes_2$ groups in acetonitrile.[13a] The reported bands were suggested to arise from acetonitrile binding to the boron atom.

The shorter wavelengths reflect negative solvatochromic shifts of 1500 cm^{-1} for **3**, 2900 cm^{-1} for **12** and 1100 cm^{-1} for **20** and parallel such shifts observed in their absorption spectra. The high-energy emission bands observed for **3**, **12** and **20** are likely to arise from formation of acetonitrile adducts where each adduct has the boron atom of the $BMes_2$ group bound to nitrogen of the acetonitrile molecule. This hypothesis is supported by computations (*vide infra*).

Comparison with the photophysical data for the reported push-pull systems **I-IV** reveals no trends or similarities between these compounds. Somewhat similar data between thiophene **12** and the dithiophene derivative **IV** are, however, noted.

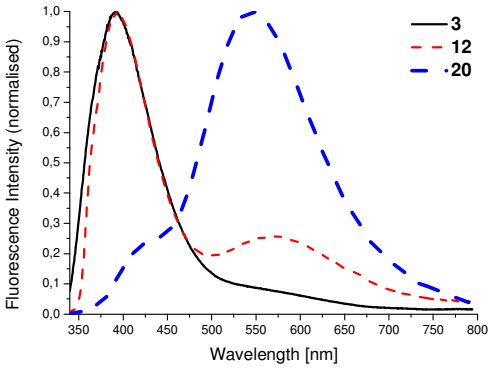

Figure 4. Emission spectra for **3**, **12** and **20** in acetonitrile.

Fluoride Species

Selected data from absorption and emission spectra recorded for the anions generated from addition of fluoride ions are listed in Table 3. The absorption maxima for these fluoride salts are higher in energies compared to their neutral species indicating that the HOMO-LUMO energy gap is increased in these salts with respect to their neutral species.

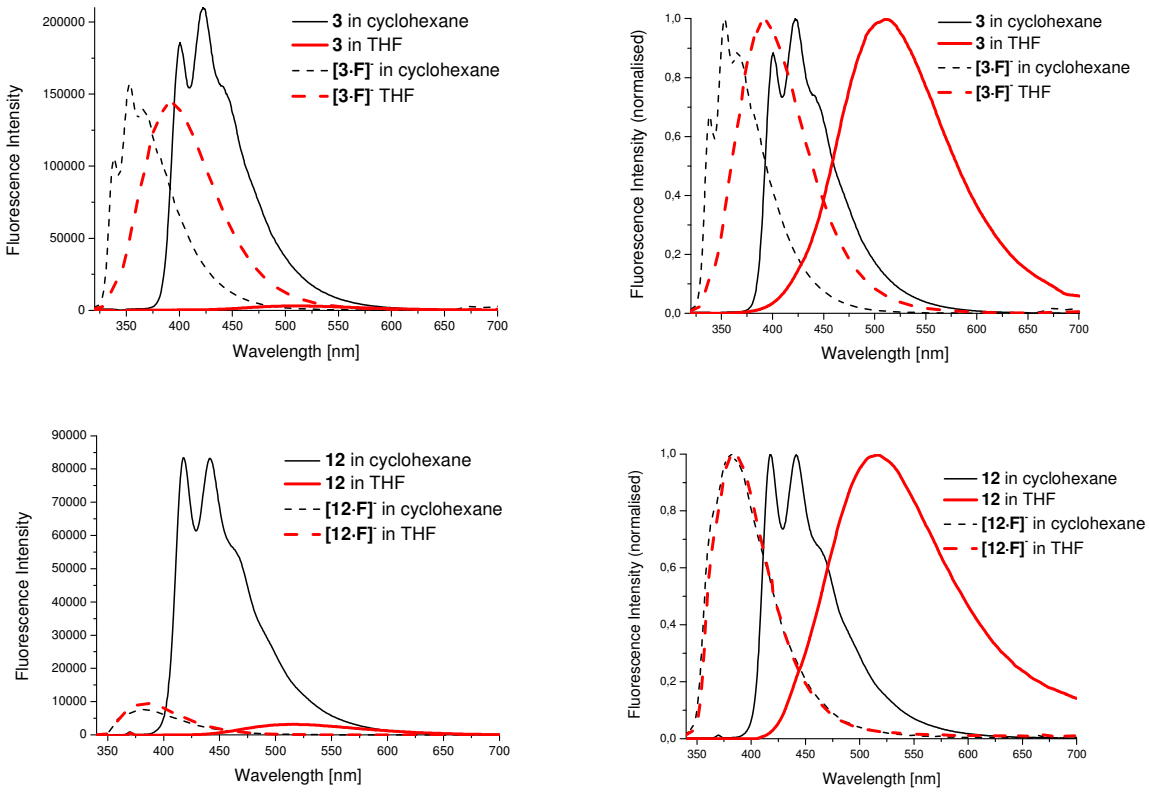

Figure 5: Emission spectra for **3** and **12** before and after fluoride addition.

Table 3. Photophysical data for the salts, [*n*Bu$_4$N][**3·F**], [*n*Bu$_4$N][**12·F**] and the anions [**20·F**]$^-$ and [**20·2F**]$^{2-}$.

	In cyclohexane solution					In THF solution					Solvatochromic shifts	
	$\lambda_{max,\ abs}$ [nm]	ε [Lmol^{-1}cm^{-1}]	$\lambda_{max,\ em}$ [nm]	Stokes shift [cm^{-1}]	Φ_{fl}	$\lambda_{max,\ abs}$ [nm]	ε [Lmol^{-1}cm^{-1}]	$\lambda_{max,\ em}$ [nm]	Stokes shift [cm^{-1}]	Φ_{fl}	absorption	emission
[3·F]$^-$	308	27600	353	4100	0.51	310	36000	393	6800	0.49	200	3100
[12·F]$^-$	331	23830	382	4000	0.07	334	29590	384	3900	0.06	100	100
[20·F]$^-$	316	33760	380	5100	0.24	318	41300	408	6900	0.26	200	2200
[20·2F]$^{2-}$	312	29040	380	5700	0.12	313	36760	401	7000	0.25	100	1400

All the fluoride salts give violet-blue fluorescence emissions with maxima between 350 and 410 nm in both cyclohexane and THF solutions. The Stokes shifts in these salts are generally lower than in their neutral analogues. The solvatochromic shifts measured on emission are varied with only 100 cm^{-1} for [**12·F**]$^-$ up to 3100 cm^{-1} for [**3·F**]$^-$ (Figure 5). Different transitions are thus likely for the two monodiazaborole anions where the excited state for [**12·F**]$^-$ is much less polar than for [**3·F**]$^-$. The observed solvatochromism of [**3·F**]$^-$ suggests a transition from the π-phenylene-ethynylene scaffold to the diazaborole unit whereas the absence of solvatochromism in **[12·F]**$^-$ points to a local π-π*-transition on the thiophene scaffold.

The photophysical data for [**3·F**]$^-$ in Table 3 are very similar to the photophysical data shown in Table 2 for the neutral derivative **V** (Chart **I**). The $BMes_2F^-$ group behaves like a spectator in the transitions involved in the low energy absorption and emission bands or like a donor such as Me and OMe in the neutral diazaboroles **VI** and **VII**, respectively, where the photophysical data are also similar. The [**3·F**]$^-$ anion may thus be viewed as an analogue of the monodiazaboroles **V**-**VI**.

One remarkable observation is the 'turn-on' fluorescence for **3** in THF on addition of fluoride anion. Compound **3** has a weak blue-green emission in THF but, on fluoride addition, an intense blue-violet emission is observed (Figure 5). The emission band intensity of **3** at 3000 units goes to 145000 units corresponding to [**3·F**]$^-$ on fluoride addition. Thus, the emission maximum intensity is increased 46 times. This 'turn-on' fluorescence is evident for **3** in THF but not in other solvents like cyclohexane (Figure 3). No such 'turn-on' fluorescence is shown for the thiophene diazaborole **12** in solvents such as THF and cyclohexane. In fact, 'turn-off' fluorescence takes place for **12** in cyclohexane with the emission intensity reduced by one-tenth and the quantum yield decreased by a factor of 6 (Figure 3).

As there are two diazaborole units with $BMes_2$ groups in **20**, it was of interest to see whether one equivalent of fluoride ion would clearly generate [**20·F**]$^-$ exclusively and whether there are unusual transitions observed between the fragment containing the anionic $BMes_2F^-$ group and that with the neutral $BMes_2$ group (Scheme 5).

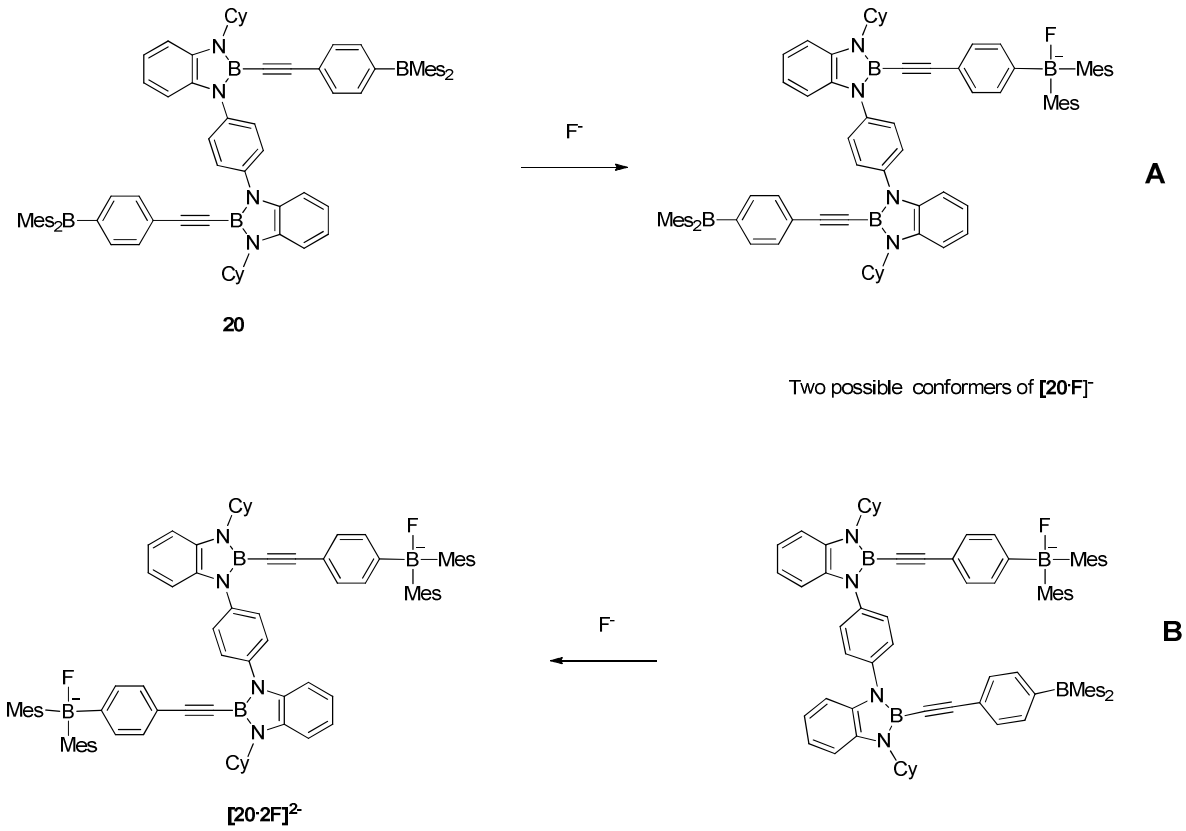

Scheme 5: Sequential fluoride addition of **20**.

Titration experiments of compound **20** with nBu$_4$NF in THF were monitored by UV-vis and fluorescence spectroscopy to examine the effect of sequential addition of fluoride ions on the bisdiazaborole. Titrations of **20** in cyclohexane with nBu$_4$NF addition were complicated by the low solubilities of the three species **20,** [**20·F**]$^-$ and [**20·2F**]$^{2-}$. Therefore, only titrations of **20** in THF solutions are discussed here.

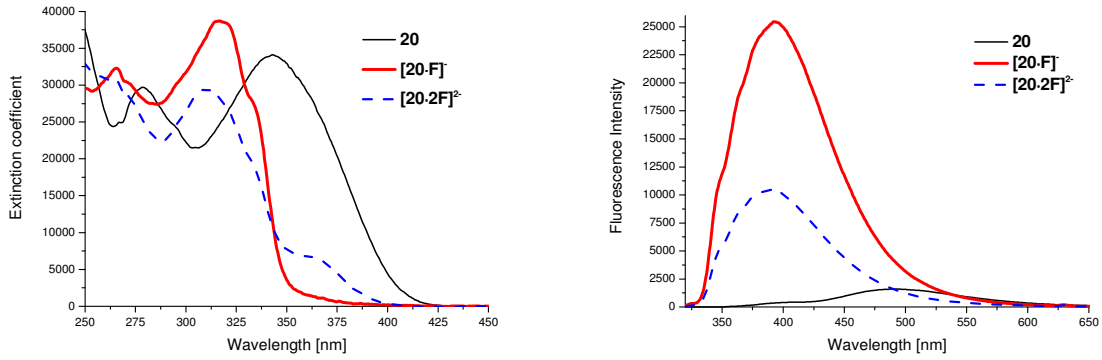

Figure 6. Absorption and emission spectra for **20**, [**20·F**] and [**20·2F**]$^{2-}$. The anions were generated by 1 and 2 equivalents of F$^-$ respectively.

Figure 6 depicts the absorption and emission spectra for the three species, **20**, [**20·F**]$^-$ and [**20·2F**]$^{2-}$ in THF where the anions were formed by addition of 1 and 2 equiv. of fluoride during the titration. Figure S3 shows the changes and isosbestic points in the absorption spectrum of **20** in THF as nBu$_4$NF is added in intervals. Addition of 1 equiv. of nBu$_4$NF leads to a blue-shift of the absorption band maximum at 343 nm for **20** to a maximum at 318 nm

assigned to the adduct **[20·F]**$^-$. Addition of a second equiv. of nBu$_4$NF gave an absorption spectrum with a maximum at 313 nm which may be assigned to the dianion **[20·2F]**$^{2-}$. In addition, a weak low-energy band appeared.

The fact that the dianion **[20·2F]**$^{2-}$ is formed from 2 equiv. of nBu$_4$NF shows that the barrier for the addition of a second fluoride ion to the monoanion **[20·F]**$^-$ is low. If [**3·F**]$^-$ is viewed as a derivative of **V** based on their photophysical data then [**20·2F**]$^{2-}$ might be compared with **16**. Indeed, Tables 2 and 3 confirm very similar values. However, on closer inspection, the neutral bisdiazaborole **16** has no low energy band at a longer wavelength than 320 nm so considering [**20·2F**]$^{2-}$ as a derivative of **16** is not straightforward here.

The monoanion **[20·F]**$^-$ has no observable absorption band at a longer wavelength than 320 nm. This is surprising as the fluoride-free part of the molecule in conformer **A** should still exhibit an absorption similar to the non perturbed precursor (Scheme 5). Such transitions would still be expected for conformer **B** where the anionic BMes$_2$F group and neutral BMes$_2$ group are in close proximity. A statistical mixture of **20**, **[20·F]**$^-$ and **[20·2F]**$^{2-}$ is expected to show a low energy band at 340-370 nm with 25% of the band intensity from **20** and 25% from **[20·2F]**$^{2-}$. Values of only 10% from **20** and 10% from **[20·2F]**$^{2-}$ were estimated assuming that there is no low energy band contribution from **[20·F]**$^-$ itself. The spectra for **[20·F]**$^-$ in Figure 6 are likely to correspond to a mixture of **20**, **[20·F]**$^-$ and **[20·2F]**$^{2-}$ where at least 90% of **[20·F]**$^-$ is present.

In the emission spectrum of **20** in THF, addition of 1 equiv. of nBu$_4$NF led to a blue-shift of the band maximum from 495 nm for **20** to 408 nm, which we assign to the adduct **[20·F]**$^-$. Two equivalents of nBu$_4$NF for one equivalent of **20** gave an emission at 401 nm corresponding to dianion **[20·2F]**$^{2-}$.

The observed emission intensity for the monoanion **[20·F]**$^-$ is at least ten-fold the emission intensity for the neutral bisdiazaborole **20** whereas the emission band intensity for the dianion **[20·2F]**$^{2-}$ is five times more intense than that of **20**. The large emission intensities of the anions compared to that of the neutral bisdiazaborole show that addition of fluoride ions also promotes fluorescence emission, i.e. 'turn-on' fluorescence, for **20** in THF. However, the relative emission intensity decreases on going from **[20·F]**$^-$ to **[20·2F]**$^{2-}$. The fluorescence intensity is clearly reduced (rather than increased as might have been expected by the two-fold fluoride addition) when the second diazaborolyl unit in **[20·F]**$^-$ is converted to the fluoride anion.

Computations

Geometry computations

Geometries of the molecules **3**, **12**, the model compound **20′** as well as the fluoride adducts **[3·F]**$^-$, **[12·F]**$^-$, **[20′·F]**$^-$ and **[20′·2F]**$^{2-}$ were optimized by DFT calculations at the B3LYP/6-31G* level of theory without any symmetry constraints. In **20′**, the cyclohexyl substituents at the nitrogen atoms of **20** were replaced by methyl groups and the *para*-methyl groups of the mesityl rings by hydrogen atoms to reduce computational efforts. The computed geometric parameters of **3**, **12** and **[12·F]**$^-$ are in reasonable agreement with the experimental geometry data (see Table S3).

For the arylethynyl systems **3**, **12**, **[3·F]**$^-$ and **[12·F]**$^-$ nearly coplanar orientations of the diazaborole units and the aryl rings with torsion angles of less than 9° were found as global minima. Rotation barriers between the rings of only 0.6 - 1.6 kcal/mol indicate that all possible rotamers may be present at ambient temperature.[27] Accordingly, the pronounced interplanar angles observed for **3**, **12** and **[12·F]**$^-$ by X-ray crystallography are likely to arise from crystal packing forces.

The geometry of **20** is considered as two molecules of **3** linked by a 'spacer' and, likewise, the geometry of **[20′·2F]**$^{2-}$ regarded as two **[3·F]**$^-$ molecules linked by a spacer. Thus,**[20′·F]**$^-$ could be viewed as containing independent molecules of **3** and **[3·F]**$^-$. The different moieties, however, suggest that there may be interactions between the two units. The most stable optimised geometry for **[20′·F]**$^-$ is the *cisoid* form where the two diazaborole-π-$BMes_2$ scaffolds are close together (conformer **B** in Scheme 5 as opposed to conformer **A** by 5.1 kcalmol^{-1}). This contrasts with the most stable conformers found for **20′** and **[20′·2F]**$^{2-}$ where *transoid* forms are adopted as given in Scheme 5. It may be argued that the different charges within the units result in favourable attraction between the two units in **[20′·F]**$^-$. Known compounds with B-F-B chelation have B-F distances of 1.49-1.64 Å. The two computed B-F distances in **20'F** are 1.48 and 4.66 Å which rule out the fluoride ion being chelated between the two boron centres here.

Molecular orbital computations

The frontier molecular orbitals for the neutral molecules **3** and **12** are depicted in Figure 7 and selected molecular orbital contributions are listed in Tables S4 and S5. As expected from earlier studies, the HOMOs of **3** and **12** are mainly located on the benzodiazaborolyl moieties whereas the LUMOs are dominated by the boron p-orbitals of the dimesitylboryl groups with contributions of the (hetero)arylene-ethynylene bridges.

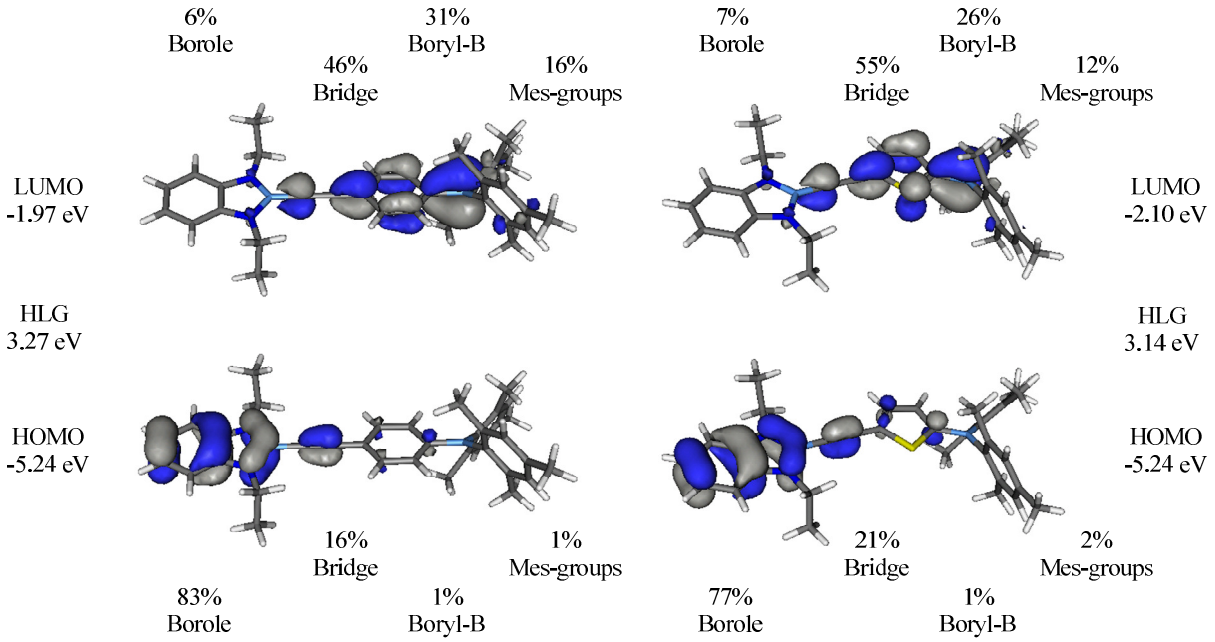

Figure 7. Frontier orbitals of compound **3** (left) and **12** (right). HLG = HOMO-LUMO-gap.

The addition of fluoride converts the electron-poor dimesitylboryl group into an electron-rich fragment. Hence, the LUMOs of the anions shown in Figure 8 are located at the phenylene-ethynylene and thiophene-ethynylene scaffolds for **[3·F]**$^-$ and **[12·F]**$^-$ respectively. The HOMOs in **[3·F]**$^-$ and **[12·F]**$^-$ are, however, very different with the HOMO located at the mesityl groups in **[3·F]**$^-$ and at the thiophene-ethynylene scaffold in **[12·F]**$^-$. Tables S6-S7 list selected molecular orbital contributions for **[3·F]**$^-$ and **[12·F]**$^-$.

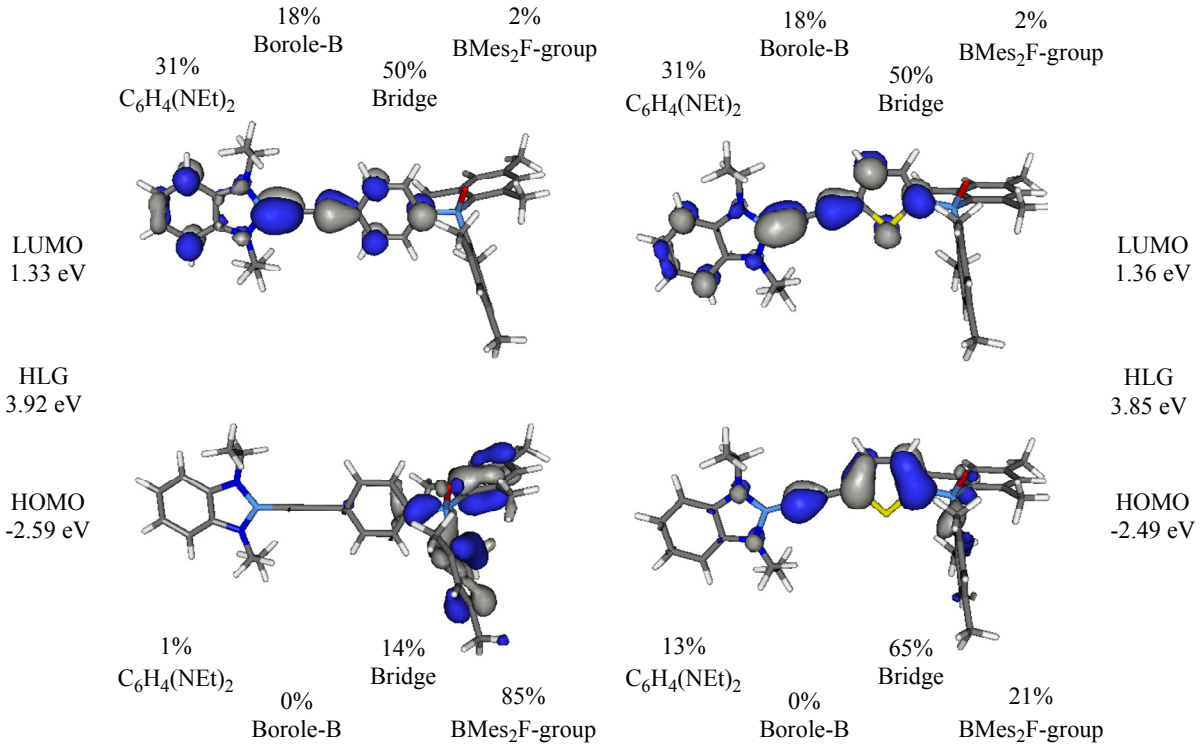

Figure 8 Frontier orbitals of fluoride adducts **[3·F]**$^-$ (left) and **[12·F]**$^-$ (right).

The molecular orbital make-ups in the N-phenylene-bridged bisboroles **20′** and its dianion **[20′·2F]**$^{2-}$are like those in the monoborolesystems **3** and **[3·F]**$^-$ respectively (Figures S4, S5; Tables S8, S9). However, the phenylene moiety contributes to 15% and 1% of the HOMO and LUMO in **20′** respectively and to 4% and 5% of the HOMO and LUMO in **[20′·2F]**$^{2-}$ respectively. These small contributions of the phenylene 'spacer' suggest that photophysical processes in **20** and **3** as well as in **[20·2F]**$^{2-}$ and **[3·F]**$^-$ are broadly similar.

The HOMO and other high lying occupied orbitals and the LUMO and other low lying unoccupied orbitals in **[20′·F]**$^-$ show even less phenylene unit contributions at ca 1% (Figure S6; Table S10). This suggests that the phenylene link is acting as a true spacer and that **[20′·F]**$^-$ is behaving like two separated chromophores, **3** and **[3·F]**$^-$.

TD-DFT calculations

Time-dependent DFT (TD-DFT) calculations at B3LYP/6-31G* on the co-planar geometries of **3**, **12**, **[3·F]**$^-$ and **[12·F]**$^-$ predict strong HOMO-LUMO transitions for **3**, **12** and **[12·F]**$^-$ but weak HOMO-LUMO transitions for **[3·F]**$^-$ (Table 4). The calculated energies of these transitions are underestimated by some 0.6 eV compared to the energies for the observed absorption maxima in cyclohexane solutions. A mixture of rotamers is expected in solution due to the very low rotation barrier between the diazaborolyl unit and the phenylene or thiophene ring so perpendicular geometries were also looked at. Calculated transition energies for the perpendicular geometries are overestimated compared to observed values (Table S11). If a mixture of rotamers is assumed to exist in solutions then agreement between experimental and computed absorption values are acceptable at the B3LYP functional. This may be fortuitous as B3LYP does not generally model long-range charge transfer transitions adequately - especially in molecules where the HOMO-LUMO overlap is negligible.[36,37]

The CAM-B3LYP functional is considered as an appropriate method for long-range charge transfer transitions and thus TD-DFT data obtained with this functional are also listed in Table 4. The calculated excitation energies are overestimated by only 0.11-0.18 eV compared to observed absorption maxima. If we take into account that a mixture of rotamers exist in solution then the calculated excitation energies from the mixture would be considerably overestimated (Table S11, also see Tables S12-S14 for MO compositions of perpendicular geometries). Nevertheless, and more importantly, the trend between observed and calculated values is excellent with the CAM-B3LYP functional.

The first vertical excitation transitions predicted from the CAM-B3LYP functional are varied. Figure 9 and Table 4 show that only in the case of **[12·F]**$^-$, the HOMO > LUMO transition is dominant and corresponds to a local π > π* transition on the thiophene-ethynylene bridge. The dominant contribution to the S_0> S_1 transition for **[3·F]**$^-$ at CAM-B3LYP is the HOMO-2 > LUMO transition which is also a local π > π* transition on the bridge along with substantial HOMO > LUMO charge transfer character. For **3** and **12**, the nature of the first vertical excitations are similar with dominant charge transfer HOMO > LUMO contributions (π borolyl > π *-bridge/boryl) and substantial local π-aryl/boryl > π*-bridge/boryl contributions.

Although the CAM-B3LYP TD-DFT data are appropriate for comparison with absorption data, the nature of these transitions computed may apply to observed emission data provided that the S_0 and S_1 geometries and their MOs are assumed to be similar. The small solvatochromic behaviour observed for **[12·F]**$^-$ compared to **[3·F]**$^-$ is supported by the absence of charge transfer character predicted for **[12·F]**$^-$. The substantial solvatochromic shifts observed in the emission data for **3** and **12** are in agreement with the dominant charge-transfer transitions predicted for **3** and **12** by CAM-B3LYP.

Table 4. TD-DFT data for the first vertical excitation using B3LYP and CAM-B3LYP functionals

	Obs.	Calc. B3LYP			Calc. CAM-B3LYP		
	λ_{max} (eV)	λ_{max} (eV)	Osc. Str.	Major transition (κ_{ia})	λ_{max} (eV)	Osc. Str.	Major transitions
3	3.63	2.95	0.63	HOMO → LUMO (0.93)	3.81	1.16	HOMO → LUMO (0.56)HOMO-3 → LUMO (0.30)
12	3.34	2.81	0.70	HOMO → LUMO (0.90)	3.52	1.38	HOMO → LUMO (0.59) HOMO-2 → LUMO (0.29)
[3·F]$^-$	4.03	3.49	0.12	HOMO → LUMO (0.69)	4.20	1.08	HOMO → LUMO (0.35) HOMO-2 → LUMO (0.54)
[12·F]$^-$	3.75	3.46	0.72	HOMO → LUMO (0.81)	3.86	1.12	HOMO → LUMO (0.65)

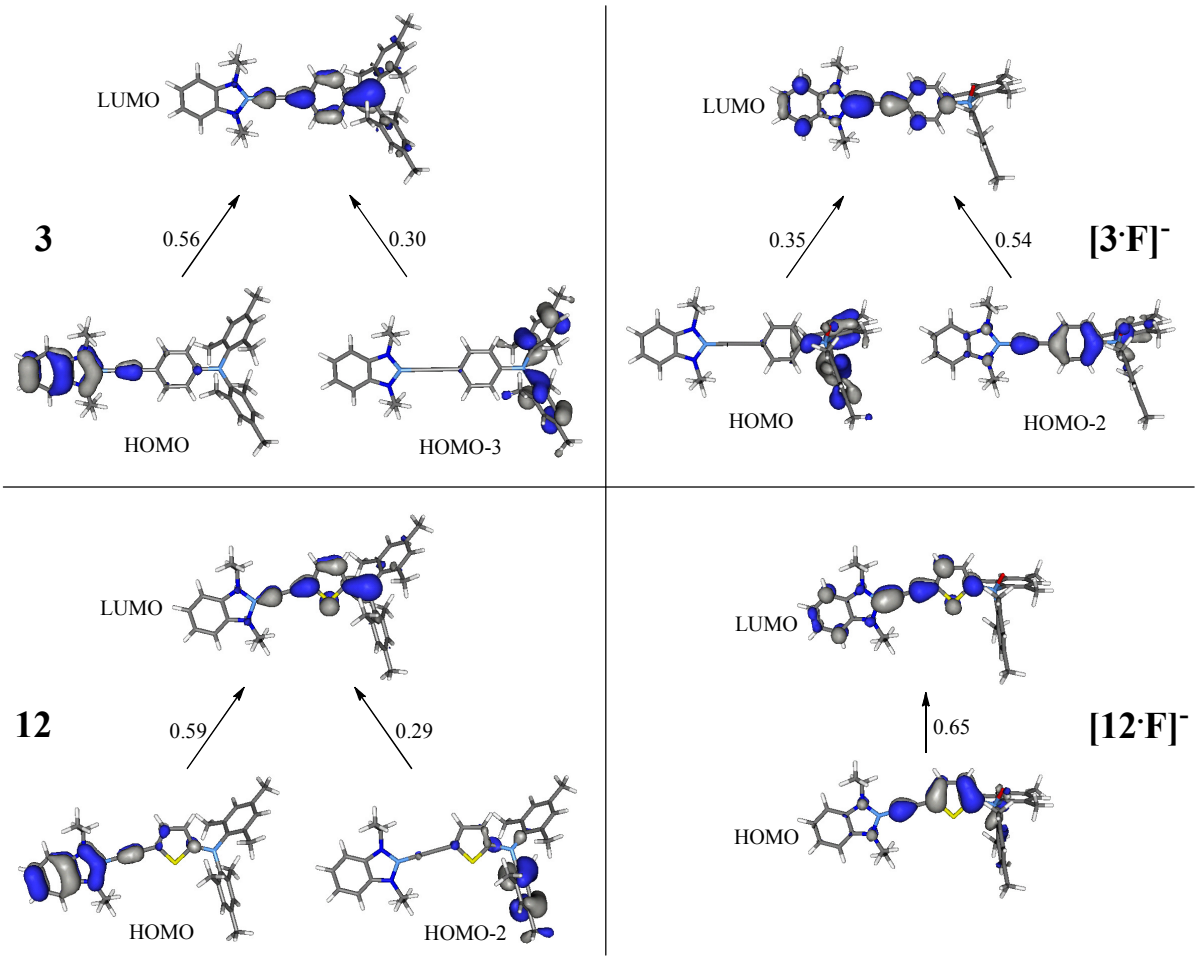

Figure 9. Orbital transitions for **3**, **12**, **[3·F]**$^-$ and **[12·F]**$^-$ with corresponding κ_{ia} value for the CAM-B3LYP functional.

Fluoride ion affinities

The affinities of compounds, **3**, **12** and **20′**, towards fluoride anions were calculated and compared with selected molecules in Charts I and II (Table 5). Fluoride anion additions of diazaboroles **III**, **IV**, **VI**, **XI**-**XIV** have been explored by spectroscopic means but no salts were isolated.[24,25] Detailed fluoride additions have been carried out on diboron compounds (Chart II, **XV**-**XIX**) with various bridges between the two $BMes_2$ groups elsewhere.[4j] These are looked at here for comparison with the bisdiazaborole **20** to estimate the affinity strengths of the second $BMes_2$ group towards the fluoride anion.

For those representatives with only $BMes_2$-groups, the first fluoride ion affinities ranged from 117.3 kcal/mol in **XVIII** to 119.2 kcal/mol in 1,4-bis(dimesitylboryl)benzene (**XVI**). These values clearly exceed the fluoride ion affinities in 1,3,2-benzodiazaborole derivatives**V**, **VI** and **XI**-**XIV** (96.1-105.3 kcal/mol). The first fluoride ion affinities in compounds **3**, **12** and both conformers **20′(A)** and **20′(B)**, where the fluoride is added to the $BMes_2$ group, are 113.3-119.1 kcal/mol in accordance with our experimental findings.

For the addition of a second F^- ion to the second $BMes_2$ substituent incompounds **XV**-**XVIII** lower fluoride ion affinities of 61.2-84.0 kcal/mol were calculated. For **20′**, the second fluoride ion affinities of 97.3-106.0 kcal/mol were found and support the facile fluoride addition of $[\mathbf{20{\cdot}2F}]^{2-}$ from $[\mathbf{20{\cdot}F}]^-$ observed here.

The second fluoride addition to compounds **3**, **12** and **I**-**IV** goes to the boron atom in the benzodiazaborole ring with low fluoride ion affinities of 47.9-65.3 kcal/mol. The values of 47.9 kcal/mol for **III** and 65.3 for **IV** are in accord with reported[24] experimental data for **III** and **IV** where the second fluoride could not be added to the borolyl group of **III** and 41 equivalents of fluoride were required to ensure the second fluoride addition to **IV**.

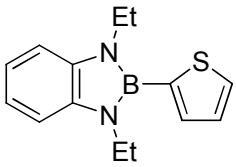

XI[24]

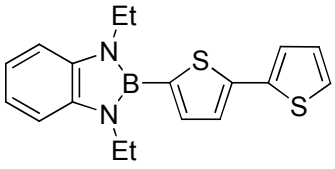

XII[24,25]

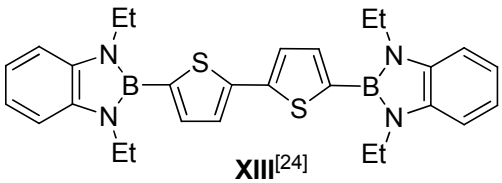

XIII[24]

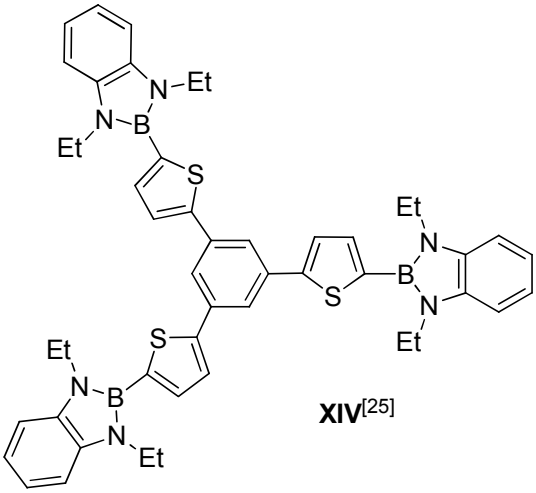

XIV[25]

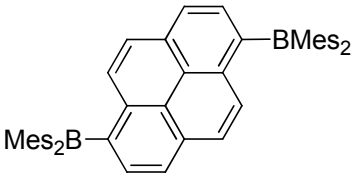

XV[5j]

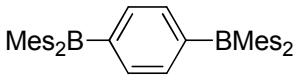

XVI[5j]

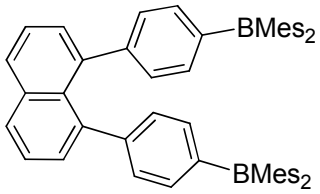

XVII[5j]

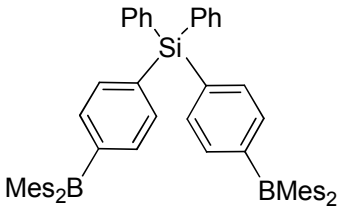

XVIII[5j]

Chart II

Table 5. Calculated fluoride ion affinities in kcal mol^{-1} for **3**, **12**, **20′** and related systems. $Et_2bdb = C_6H_4(NEt)_2B$-, Mebdb = μ-$N(C_6H_4NMe)B$-, Th = 2-C_4H_3S

Compound		1st F^-	2nd F^-
Et_2bdb-CC-1,4-C_6H_4-$BMes_2$	**3**	118.0	56.2
Et_2bdb-CC-2,5-C_4H_2S-$BMes_2$	**12**	118.1	54.4
1,4-[Mebdb-CC-1',4'-C_6H_4-$BMes_2$]$_2C_6H_4$ via conformer **A**	**20′**	113.3	106.0
1,4-[Mebdb-CC-1',4'-C_6H_4-$BMes_2$]$_2C_6H_4$via conformer **B**	**20′**	119.1	97.3
Et_2bdb-1,4-C_6H_4-$BMes_2$	**I**	116.7	48.4
Et_2bdb-1,4-C_6H_4-1,4-C_6H_4-$BMes_2$	**II**	116.8	64.7
Et_2bdb-2,5-C_4H_2S-$BMes_2$	**III**	115.8	47.9
Et_2bdb-2,5-C_4H_2S-2,5-C_4H_2S-$BMes_2$	**IV**	115.3	65.3
Et_2bdb-CC-Ph	**V**	96.7	-
Et_2bdb-CC-C_6H_4Me	**VI**	96.1	-
Et_2bdb-Th	**XI**	99.7	-
Et_2bdb-2,5-C_4H_2S-Th	**XII**	103.2	-
Et_2bdb-2,5-C_4H_2S-2,5-C_4H_2S-Et_2bdb	**XIII**	105.0	64.0
1,3,5-(Et_2bdb-2',5'-C_4H_2S)$_3C_6H_3$	**XIV**	105.3	75.1
Mes_2B-1,6-$C_{14}H_8$-$BMes_2$	**XV**	118.6	72.4
Mes_2B-1,4-C_6H_4-$BMes_2$	**XVI**	119.2	61.2
Mes_2B-1,4-C_6H_4-1,8-$C_{10}H_6$-1,4-C_6H_4-$BMes_2$	**XVII**	117.3	73.3
Mes_2B-1,4-C_6H_4-$SiPh_2$-1,4-C_6H_4-$BMes_2$	**XVIII**	118.0	84.0

The influence of acetonitrile as solvent in 3, 12 and 20

The photophysical data for **3**, **12** and **20** in acetonitrile solutions revealed absorption and emission bands with negative solvatochromic shifts. Such behaviour has been observed for other push-pull systems involving $BMes_2$ groups as acceptors elsewhere.[13a] One possibility is that 1:1 acetonitrile adducts exist in solution where the acetonitrile is weakly bound via nitrogen to the boron atom in the $BMes_2$ group which had been suggested previously.[13a]

The acetonitrile affinities of **3** and **12** based on the optimised geometries of **3·NCMe** and **12·NCMe** adducts are only 10.4 and 12.0 $kcalmol^{-1}$, respectively. TD-DFT data on these adducts at the CAM-B3LYP functional (**3·NCMe** 4.25 eV; **12·NCMe** 3.98 eV) resemble that of the anions **[3·F]**$^-$ and **[12·F]**$^-$ (Table 4). However, the observed absorption bands for **3** and **12** in acetonitrile (3.71 and 3.51 eV respectively) are not close to the CAM-B3LYP energies. The ^{11}B NMR data of **3** and **12** in CD_3CN solutions where the two resonances are observed are as expected for the neutral species. At the ground states, compounds **3** and **12** are relatively polar (more stabilised in more polar solvents) and thus negative solvatochromic shifts are observed in the absorption spectra.

One argument for the unusual emission data of **3** and **12** observed here in acetonitrile is that mixtures of both the neutral species and the weakly-bound acetonitrile adduct exist as the

acetonitrile affinities of **3** and **12** in the excited states may be substantial unlike in the ground states. The high-energy emission bands of 391 and 394 nm in **3** and **12** respectively (Figure 4) correspond to the weakly-bound **3·NCMe** and **12·NCMe** adducts partly because these adducts have much higher fluorescence intensities than **3** and **12** in acetonitrile. Compounds **3** and **12** have low quantum yields in acetonitrile with Φ_{fl} values of 0.03 at 550 nm for **3** and 0.08 at 567 nm for **12**. When excited at the high-energy emission wavelengths, the observed excitation spectra are different from the absorption spectra of **3** and **12** with the band maxima at 310 and 325 nm from acetonitrile solutions of **3** and **12** respectively. These excitation spectra are likely to correspond to **3·NCMe** and **12·NCMe** as the respective values of 4.00 eV and 3.80 eV are in good agreement with the calculated CAM-B3LYP values of 4.25 eV and 3.98 eV for these adducts respectively.

The much weaker high-energy emission band observed for **20·NCMe** relative to **20** suggests that i) the acetonitrile affinity for the excited state of **20** is lower than the affinities for the excited states of **3** and **12** or ii) the fluorescence intensity for **20·NCMe** is low or iii) both. Nevertheless, when excited at the high-energy emission wavelength, the observed excitation spectrum has a band at 317 nm which is likely to arise from the acetonitrile adduct, **20·NCMe**.

Conclusions

It has been demonstrated that 1,3,2-benzodiazaboroles functionalized by phenylene-ethynylene- and thiophene-ethynylene groups (**3**, **5**, **12**, **16** and **20**) with electron-attracting units like $BMes_2$ and CN can be synthesized by known methodologies. All were fluorescent with emission maxima of 379-441 nm and quantum yields up to Φ_{fl} = 0.99 in cyclohexane. Addition of fluoride ion to the push-pull benzodiazaboroles with -$BMes_2$ groups (**3**, **12** and **20**) gave anions containing -$BFMes_2$ groups. These fluoride adducts had emission maxima considerably blue-shifted relative to their neutral species and, for **3** and **20** in THF solutions, 'turn-on' fluorescence was observed on fluoride ion addition. The push-pull systems revealed emission maxima at 391-410 nm in acetonitrile suggesting that adducts exist with the boron in the $BMes_2$ group bound to acetonitrile. Further studies on other benzodiazaborole-boryl systems as 'turn-on' fluoride sensors are in progress.

Experimental section

General: All manipulations were performed under dry, oxygen-free argon by using Schlenk techniques. Solvents were dried by standard methods and freshly distilled prior to use. The compounds 2-bromo-1,3-diethyl-1,3,2-benzodiazaborole (**1**),[16] 4-dimesitylboryl-phenylacetylene (**2**),[30] 4-cyanophenylacetylene (**4**),[31] (2-trimethylsilylethynyl)thiophene (**8**),[32] dimesityl fluoroborane (**9**)[33] and 1,3-bis(2´,6´-diisopropylphenyl)imidazolium chloride[34] were prepared according to literature methods. 4-Bromobenzonitrile (**6**), 2-bromoaniline, *p*-phenylenediamine, boron tribromide, sodium tetrahydridoborate, palladium acetate and tetrabutylammonium fluoride trihydrate (TBAF·$3H_2O$) were purchased commercially. Titration experiments were performed with a commercially available tetrabutylammonium fluoride solution (1 M in THF).

NMR spectra were recorded at room temperature with a Bruker AM Avance DRX-500 spectrometer {^{1}H, ^{11}B, ^{13}C} by using TMS and BF_3·OEt_2 as external standards. Mass spectra were taken with a VG autospec sector field mass spectrometer (Micromass).
Absorption spectra were measured with a UV/VIS double-beam spectrometer (Shimadzu UV-2550). The setup used to acquire excitation-emission spectra (EES) was similar to that employed in commercial static fluorimeters: the output of a continuous Xe-lamp (75W, LOT Oriel) was wavelength-separated by a first monochromator (Spectra Pro ARC-175, 1800 l/mm grating, Blaze 250 nm) and then used to irradiate a sample. The fluorescence was collected by mirror optics at right angles and imaged on the entrance slit of a second spectrometer while compensating astigmatism at the same time. The signal was detected by a back-thinned CCD camera (RoperScientific, 1024 × 256 pixels) in the exit plane of the spectrometer. The resulting images were spatially and spectrally resolved. As the next step, one averaged fluorescence spectrum was calculated from the raw images and stored in the computer. This process was repeated for different excitation wavelengths. The result is a two-dimensional fluorescence pattern with the *y*-axis corresponding to the excitation, and the *x*-axis to the emission wavelength. A wavelength range of λ_{ex} = 230–450 nm (in 1 nm increments) for the excitation and λ_{em} = 200–800 nm for the detection was employed. The time to acquire a complete EES is typically less than 15 min. Post-processing of the EES includes subtraction of the dark current background, conversion of pixel to wavelength scales, and multiplication with a reference file to take the varying lamp intensity as well as grating and detection efficiency into account. For all measurements, samples were contained in quartz cuvettes of 10 × 10 mm^2 (Hellma type 111-QS, suprasil, optical precision). They were prepared with distilled and dried THF or cyclohexane, with concentrations varying from 1 to 8 μM according to their optical density. The quantum yields were determined using POPOP (p-bis-5-phenyl-oxazolyl(2)-benzene) (Φ_{fl} = 0.93) as the standard.

2(4'-Dimesitylboryl-phenylethynyl)-1,3-diethyl-1,3,2-benzodiazaborole (3): A solution of 4-dimesitylboryl-phenylacetylene (**2**) (0.62 g, 1.77 mmol) in *n*-hexane (20 mL) was added dropwise with 1.11 mL (1.77 mmol) of 1.6 M solution of *n*-butyllithium in *n*-hexane at 20 °C. After 30 min of stirring neat 2-bromo-1,3-diethyl-1,3,2-benzodiazaborole (**1**) (0.44 g, 1.77 mmol) was added. The mixture was stirred for 16 h at room temperature. It was filtered. The filtrate was concentrated until it became cloudy and cooled overnight at -20 °C. Compound **3** separated as colourless platelets (0.83 g, 90% yield). ^{1}H-NMR (C_6D_6), δ = 1.20 (t, $^{3}J_{HH}$ = 7.2 Hz, 6H, CH_2CH_3), 2.10 (s, 12H, *o*-CH_3-mesityl), 2.20 (s,6H, *p*-CH_3-mesityl), 3.75 (q, $^{3}J_{HH}$ = 7.2 Hz, 4H, CH_2CH_3), 6.79 (s, 4H, CH-mesityl), 6.95 (m, 2H, diazaborolyl C*H*=CH-CH=C*H*), 7.12 (m, 2H, diazaborolyl CH=C*H*-C*H*=CH), 7.57 (m, 4H, H-phenylene) ppm. ^{13}C{^{1}H}-NMR (C_6D_6): δ= 15.9 (s, CH_2CH_3), 21.0 (s, *p*-CH_3-mesityl), 23.4 (s, *o*-CH_3-mesityl), 38.1 (s, CH_2CH_3), 107.0 (s, B-C≡*C*), 109.1 (s, diazaborolyl *C*H=CH-CH=*C*H), 119.3 (s, diazaborolyl CH=*C*H-*C*H=CH), 126.6 (s, C≡C-*C*), 128.6 (s, CH-mesityl), 131.6 (s, CH-phenylene), 136.1 (s, CH-phenylene), 136.9 (s, diazaborolyl C_2N_2), 138.6 (s, *p*-C-mesityl), 140.7 (s, *o*-C-mesityl),141.6 (s, BC-mesityl), 146.7 (s, BC-phenylene) ppm. The borolyl B-*C*≡C peak was not observed. ^{11}B{^{1}H} NMR (C_6D_6): δ = 21.1 (s, BN_2), 74.4 (s, $BMes_2$) ppm. MS/EI: m/z (%) = 522.5(100), $[M]^+$, 402.4(35), M^+-MesH, 387.4(33) M^+-MesH-CH_3. $C_{36}H_{40}B_2N_2$ (522.34): calcd. C 82.78, H 7.72, N 5.36; found C 82.74, H 7.84, N 5.34.

Formation of [*n*Bu$_4$N][3·F]$^-$: Equimolar amounts of **3** (27.5 mg, 0.053 mmol) and tetrabutylammonium fluoride trihydrate (TBAF·3H$_2$O) (18.3 mg, 0.058 mmol) were dissolved in 0.8 mL of C_6D_6. Layering the solution with 4 mL *n*-pentane gave the 1:1 adduct as a colourless solid. ^{1}H NMR (C_6D_6): δ = 0.78 (t, $^3J_{HH}$ = 7.5 Hz, 12H, $(CH_2)_3CH_3$), 1.03 (m, 16H, $CH_2CH_2CH_2CH_3$), 1.24 (t, $^3J_{HH}$ = 7.2 Hz, 6H, CH_2CH_3), 2.30 (s, 6H, *p*-CH_3-mesityl), 2.34 (m, 8H, $CH_2(CH_2)_2CH_3$), 2.45 (s, 12H, *o*-CH_3-mesityl), 3.82 (q, $^3J_{HH}$ = 7.2 Hz, 4H, CH_2CH_3), 6.84 (s, 4H, H-mesityl), 6.96 (m, 2H, diazaborolyl C*H*=CH-CH=C*H*), 7.10 (m, 2H, diazaborolyl CH=C*H*-C*H*=CH), 7.73 (m, 4H, H-phenylene) ppm. ^{11}B{^{1}H} NMR (C_6D_6): δ = 5.1 (s, 1B, $BMes_2F$), 21.3 (s, 1B, BN_2) ppm. ^{19}F{^{1}H} NMR (C_6D_6): -172.2 (s) ppm.

2(4'-Cyanophenylethynyl)-1,3-diethyl-1,3,2-benzodiazaborole (5): The solution of 4-cyanophenylacetylene (0.26 g, 2.05 mmol) in 15 mL of THF was combined at 20 °C with the solution of an equimolar amount of $LiN(SiMe_3)_2$, freshly made from 0.33 g $HN(SiMe_3)_2$ (2.05 mmol) and 1.28 mL (2.05 mmol) of a 1.6 M *n*-butyllithium solution in *n*-hexane. Stirring of the resulting black solution was continued for 30 min, before a sample of **1** (0.51 g, 2.05 mmol) was added. After 16 h of stirring the solvents and all volatile components were removed *in vacuo*. The solid residue was triturated with 30 mL of warm *n*-hexane (ca. 60 °C) and filtered. Storing the filtrate overnight at -35 °C afforded 0.42 g (69% yield) of product **5** as colourless needles. ^{1}H-NMR (C_6D_6): δ = 1.20 (t, $^3J_{HH}$ = 7.2 Hz, 6H, CH_2CH_3), 3.73 (q,^{3} J_{HH} = 7.2 Hz, 4H, CH_2CH_3), 6.84 (d, $^3J_{HH}$ = 8.2 Hz, 2H, H-phenylene), 6.95 (m, 2H, diazaborolyl, C*H*=CH-CH=C*H*), 7.04 (d, $^3J_{HH}$ = 8.2 Hz, 2H, H-phenylene), 7.12 (m, 2H, diazaborolyl CH=C*H*-C*H*=CH) ppm. ^{13}C{^{1}H}-NMR (C_6D_6): δ = 16.1 (s, CH_2CH_3), 38.3 (s,CH_2CH_3), 104.9 (s, B-C≡*C*), 109.4 (s, diazaborolyl *C*H=CH-CH=*C*H), 112.3 (s, *C*-CN), 118.1 (s, C-*C*N), 119.7 (s, diazaborolyl CH=*C*H-*C*H=CH), 127.1 (s, C≡C-*C*), 131.8 (s, CH-phenylene), 132.1 (s, CH-phenylene), 136.9 (s, diazaborolyl C_2N_2) ppm. The borolyl B-*C*≡C peak was not observed. ^{11}B{^{1}H}-NMR (C_6D_6): δ = 20.7 (s) ppm. MS/EI: m/z (%) = 299.3(98), [M$^+$], 284.2(100), [M]$^+$-CH_3. $C_{19}H_{18}BN_3$ (299.18): calcd. C. 76.28, H 6.06, N 14.05; found C 75.66, H 6.38, N 13.73.

2-(Dimesitylboryl)-5-(trimethylsilylethynyl)thiophene (10): A solution of 2-(trimethylsilylethynyl)thiophene (0.80 g, 4.44 mmol) in diethyl ether (20 mL) was deprotonated at room temperature by treatment with 2.77 mL (4.44 mmol) of a 1.6 M solution of *n*-butyllithium in *n*-hexane. After 1.5 h of stirring, a solution of dimesityl fluoroborane (1.2 g, 4.44 mmol) in diethyl ether (25 mL) was added and stirring was continued for 16 h. The resulting mixture was combined with 50 mL of brine. The organic phase was separated and the aqueous phase was extracted with diethyl ether (2 x 50 mL). The combined ether phases were dried with anhydrous Na_2SO_4. After filtration the solvent was removed *in vacuo*. The residue (1.81 g, 95%) was identified by NMR spectroscopy and subsequently desilylated to give compound **11**. ^{1}H-NMR (C_6D_6): δ = 0.16 (s, 9H, $SiMe_3$), 2.15 (s, 12H, *o*-CH_3-mesityl), 2.18 (s, 6H, *p*-CH_3-mesityl), 6.76 (s, 4H, *m*-H-mesityl), 7.12 (d, $^3J_{HH}$ = 1.9 Hz, 1H, H-thiophene), 7.13 (d, $^3J_{HH}$ = 1.9 Hz, H-thiophene) ppm. ^{13}C{^{1}H} NMR (C_6D_6): δ = -0.5 [s, $Si(CH_3)_3$], 21.1 (s, *p*-CH_3-mesityl), 23.4 (s. *o*-CH_3-mesityl), 98.4 (s, C≡*C*-$SiMe_3$), 102.8 (s, *C*≡C-$SiMe_3$), 128.7 (s, CH-mesityl), 134.4 (s, CH-thiophene), 136.4 (s, C-thiophene), 138.8

(s, *p*-C-mesityl), 139.9 (s, CH-thiophene), 140.8 (s, *o*-C-mesityl), 141.2 (s, BC-mesityl), 152.7 (s, BC-thiophene) ppm. $^{11}B\{^1H\}$ NMR (C_6D_6): δ = 65.2 ppm.

2-(Dimesitylboryl)-5-(ethynyl)thiophene (11): A sample of K_2CO_3 (2 g) was added to the solution of compound **10** (1.81 g, 4.22 mmol) in a mixture of CH_2Cl_2 (50 mL) and methanol (50 mL). After stirring the slurry for 3 h at 20 °C water (100 mL) was added. The aqueous layer was extracted with CH_2Cl_2 (2x50 mL). The combined organic layers were dried (Na_2SO_4) and then filtered. Solvent was evaporated *in vacuo* and the residue was chromatographed on Silica 60 (Merck) in a short column (l = 30 cm, Ø = 5 cm) with cyclohexane as an eluent. Product **11** was isolated as a yellow solid (0.93 g, 62% yield). ^{1}H-NMR (C_6D_6): δ = 2.15 (s, 12H, *o*-CH_3-mesityl), 2.18 (s, 6H, *p*-CH_3-mesityl), 2.98 (s, 1H, C≡CH), 6.76 (s, 4H, *m*-H-mesityl), 7.08 (d, $^3J_{HH}$ = 3.8 Hz, 1H, H-thiophene), 7.12 (d, $^3J_{HH}$ = 3.8 Hz, 1H, H-thiophene) ppm. $^{13}C\{^1H\}$ NMR (C_6D_6): δ = 21.1 (s, *p*-CH_3-mesityl), 23.4 (s, *o*-CH_3-mesityl), 77.1 (s, C≡*C*H), 85.0 (s, *C*≡CH), 128.6 (s, CH-mesityl), 134.2 (s, C≡C-*C*), 134.9 (s, CH-thiophene), 138.9 (s, *p*-C-mesityl), 139.8 (s, CH-thiophene), 140.8 (s, *o*-C-mesityl), 141.2 (s, BC-mesityl), 152.8 (s, BC-thiophene) ppm. $^{11}B\{^1H\}$ NMR (C_6D_6):δ = 65.9 ppm.

2-(5'-Dimesitylboryl-2'-thienylethynyl)-1,3-diethyl-1,3,2-benzodiazaborole (12): The solution of **11** (0.73 g, 2.05 mmol) in *n*-hexane (25 mL) was treated at room temperature with 1.28 mL (2.05 mmol) of a 1.6 M solution of *n*-butyllithium in *n*-hexane. After 30 min 0.80 g (3.17 mmol) of neat **1** was added and stirring was continued for 16 h. The slurry was filtered and the filter-cake was washed with hot *n*-hexane (ca. 60 °C). The filtrate was freed from all volatile components. Crystallization of the crude material from *n*-hexane yielded 0.58 g (54%) of product **12** as large colourless crystals. ^{1}H-NMR (C_6D_6): δ = 1.14 (t, $^3J_{HH}$ = 7.2 Hz, 6H, CH_2CH_3), 2.19 (s, 6H, *p*-CH_3-mesityl), 2.20 (s, 12H, *o*-CH_3-mesityl), 3.69 (q, $^3J_{HH}$ = 7.2 Hz, 4H, CH_2CH_3), 6.78 (s, 4H, H-mesityl), 6.92 (m, 2H, diazaborolyl C*H*=CH-CH=C*H*), 7.09 (m, 2H, diazaborolyl CH=C*H*-C*H*=CH), 7.21 (d, $^3J_{HH}$ = 3.9 Hz, 1H, H-thiophene), 7.23 (d, $^3J_{HH}$ = 3.9 Hz, 1H, H-thiophene) ppm. $^{13}C\{^1H\}$-NMR (C_6D_6): δ = 16.0 (s, CH_2CH_3), 21.1 (s, *p*-CH_3-mesityl), 23.5 (s, *o*-CH_3-mesityl), 38.3 (s, CH_2CH_3), 99.6 (s, B-C≡*C*), 109.3 (s, diazaborolyl *C*H=CH-CH=*C*H), 119.5 (s, diazaborolyl CH=*C*H-*C*H=CH), 128.7 (s, CH-mesityl), 134.7 (s, CH-thiophene), 136.6 (s, C≡C-*C*), 137.0 (s, C_2N_2), 138.9 (s, *p*-C-mesityl), 140.1 (s, CH-thiophene), 140.9 (s, *o*-C-mesityl), 141.2 (s, BC-mesityl), 153.2 (s, BC-thiophene) ppm. The borolyl B-*C*≡C peak was not observed. $^{11}B\{^1H\}$-NMR (C_6D_6): δ = 20.9 (s, BN_2), 66.8 (s, $BMes_2$) ppm. MS/EI: m/z (%) = 528.3(100) $[M]^+$, 408.2(23), $[M]^+$-MesH, 393.1(18) $[M]^+$-MesH-CH_3. $C_{34}H_{38}B_2N_2S$ (528.37): calcd. C 77.29, H 7.25, N 5.30; found C 75.84, H 7.41, N 5.26.

Formation of [*n*Bu_4N][12·F]: Equimolar amounts of **12** (21.5 mg, 0.04 mmol) and TBAF·$3H_2O$ (15.4 mg, 0.049 mmol) were combined in C_6D_6 (0.8 mL). Layering the clear solution with *n*-pentane (3 mL) gave the 1:1 adduct as colourless crystals. ^{1}H-NMR (C_6D_6): δ = 0.83 (t, $^3J_{HH}$ = 7.5 Hz, 12H, $(CH_2)_3CH_3$), 1.06 (m, 16H, CH_2 $CH_2CH_2CH_3$), 1.24 (t, $^3J_{HH}$ = 7.2 Hz, 6H, CH_2CH_3), 2.29 (s, 6H, *p*-CH_3-mesityl), 2.35 (m, 8H, $CH_2(CH_2)_2CH_3$), 2.53 (s, 12H, *o*-CH_3-mesityl), 3.81 (q, $^3J_{HH}$ = 7.2 Hz, 4H, CH_2CH_3), 6.83 (s, 4H, H-mesityl), 6.96 (m,

2H, C*H*=CH-CH=C*H*), 7.03 (m, 1H, H-thiophene), 7.10 (m, 2H, CH=C*H*-C*H*=CH), 7.43 (m, 1H, H-thiophene) ppm. $^{11}B\{^1H\}$-NMR (C_6D_6): δ = 5.0 (s, 1B, $BMes_2F$), 21.4 (s, 1B, BN_2) ppm. $^{19}F\{^1H\}$-NMR (C_6D_6): -163.1 (s) ppm.

2-Isopropylamino-1-bromobenzene (13): Molecular sieves (20 g, 3 Å) were added to a solution of 2-bromoaniline (15.0 g, 87.2 mol) in acetone (150 mL) and the resulting mixture was vigorously stirred for 24 h. It was filtered and the filtrate was evaporated to dryness to afford a yellow oil. $NaBH_4$ (9.9 g, 261.6 mmol) was added at 0 °C to a solution of this oil in methanol (150 mL). The reaction mixture was stirred for 16 h, during which the ice bath warmed up to ambient temperature. Then 150 mL of a 1 M aqueous NaOH solution was added. The resulting mixture was extracted with CH_2Cl_2 (3x100 mL) and the combined organic layers were dried with anhydrous Na_2SO_4. After removal of solvents the residue was purified by short path distillation ($2x10^{-5}$ bar, 60 °C bath temperature) to give 15.6 g (84%) of product **13** as colourless liquid. ^{1}H-NMR (C_6D_6): δ = 0.88 (d, $^3J_{HH}$ = 6.3 Hz, 12H, CH(CH_3)$_2$), 3.69 (d of sept., $^3J_{HH}$ = 5.7, 6.3 Hz, 1H, C*H*(CH_3)$_2$), 4.13 (d, $^3J_{HH}$ = 5.7 Hz, 1H, NH), 6.37 (dd, $^3J_{HH}$ = 7.7 Hz, $^4J_{HH}$ = 1.4 Hz, 1H, H-phenylene), 6.40 (m, 1H, H-phenylene), 6.99 (m, 1H, H-phenylene), 7.37 (dd, $^3J_{HH}$ = 7.9 Hz, $^4J_{HH}$ = 1.3 Hz, 1H, H-phenylene) ppm.

N,N'-(bis-2'-isopropylamino-phenyl)-*p*-phenylenediamine (14): Sodium *tert*-butanolate (0.039 g, 0.40 mmol), 1,3-bis(2,6-diisopropylphenyl)imidazolium chloride (0.175 g, 0.37 mmol) and 0.041 g (0.18 mmol) of palladium acetate were dissolved with stirring in hot toluene (10 mL, 80 °C). This solution was added to a mixture of 4.00 g (36.99 mmol) of *p*-phenylenediamine, 15.84 g (73.98 mmol) of **13** and 7.11 g (73.98 mmol) of sodium *tert*-butanolate in 500 ml of toluene. The mixture was heated for 48 h at 110 °C, whereby solid NaBr separated. The dark solution was washed with a degassed saturated NH_4Cl-solution (3x150 mL) and brine (1x 150 mL) before the organic phase was dried with Na_2SO_4. Removal of solvent *in vacuo* gave a dark blue oil. This oil was crystallized twice from toluene to yield product **14** (9.80 g, 71.0%) as colourless crystals. ^{1}H-NMR (C_6D_6): δ = 0.92 (d, $^3J_{HH}$ = 6.3 Hz, 12H, CH(CH_3)$_2$), 3.37 (sept., $^3J_{HH}$ = 6.3 Hz, 2H, C*H*(CH_3)$_2$), 3.85 (s, 2H, NH), 4.43 (s, 2H, NH), 6.53 (s, 4H, 1,4-phenylenediamine C=C*H*-C*H*=C), 6.67, 6.72, 7.04, 7.09 (4m, 8H, CH-CH=CH-CH) ppm. $^{13}C\{^1H\}$-NMR (C_6D_6): δ = 22.7 (s, CH(*C*H_3)$_2$), 43.8 (s, *C*H(CH_3)$_2$), 111.9 (s, CH-1,2-phenylenediamine), 117.3 (s, CH-1,2-phenylenediamine), 118.0 (s, 1,4-phenylenediamine C=*C*H-*C*H=C), 123.3 (s, CH-1,2-phenylenediamine), 125.1 (s, CH-1,2-phenylenediamine), 130.8 (s, 1,4-phenylenediamine *C*=CH-CH=*C*), 139.0 (s, C-1,2-phenylenediamine), 142.5 (s, C-1,2-phenylenediamine) ppm. MS/EI: m/z (%)= 374.3(100) [M^+], 288.1(29) [M^+-2CH(CH_3)$_2$]. $C_{24}H_{30}N_4$(374.52): calcd. C 76.97, H 8.07, N 14.96; found C 77.17, H 8.02, N 14.93.

1,4-Bis[(2'-bromo-3'-isopropyl-1',3',2'-benzodiazaborol-1'-yl)]benzene (15): A slurry of calcium hydride (2.80 g, 66.0 mmol) in CH_2Cl_2 (50 mL) was simultaneously combined with two separate solutions of **14** (5.00 g, 13.35 mmol) and boron tribromide (7.34 g, 29.37 mmol) each in 50 mL of CH_2Cl_2. The slurry was stirred 16 h at room temperature, then filtered and the filtrate was liberated from volatile components *in vacuo*. The residue was crystallized from toluene to give product **15** (4.50 g, 61%) as colourless crystals. Single crystals of the

material were grown by layering a saturated $CHCl_3$ solution with *n*-pentane. ^{1}H-NMR (C_6D_6): δ = 1.55 (d, $^3J_{HH}$ = 6.3 Hz, 12H, CH(C*H*$_3$)$_2$), 4.47 (sept., $^3J_{HH}$ = 6.3 Hz, 2H, C*H*(CH$_3$)$_2$), 6.93 (m, 2H, CH-diazaborolyl), 7.01 (m, 2H, CH-diazaborolyl), 7.06 (m, 2H, CH-diazaborolyl), 7.22 (m, 2H, CH-diazaborolyl), 7.38 (s, 4H, 1,4-phenylendiamine C=CH-CH=C) ppm. ^{13}C{^{1}H}-NMR (C_6D_6): δ = 21.8 (s, CH(*C*H$_3$)$_2$), 46.5 (s, *C*H(CH$_3$)$_2$), 110.8, 110.9, 119.9, 120.4 (4s, CH-diazaborolyl), 128.4 (s, 1,4-phenylendiamin C=*C*H-*C*H=C), 135.7 (s, 1,4-phenylendiamin *C*=CH-CH=*C*), 137.5, 137.6 (2s, C-diazaborolyl) ppm. The borolyl B-*C*≡C peak was not observed. ^{11}B{^{1}H}-NMR (C_6D_6): δ = 22.9 (s) ppm. $C_{24}H_{26}B_2Br_2N_4$ (551.92): calcd. C 52.23, H 4.75, N 10.15, found C 51.41, H 4.31, N 10.01.

1,4-Bis[2'-phenylethynyl-3'-isopropyl-1',3',2'-benzodiazaborol-1'-yl)]benzene (16): Lithium phenylacetylide was prepared from phenylacetylene (0.43 g, 4.19 mmol) and 2.61 mL (4.19 mmol) of a 1.6 M hexane solution of *n*-butyllithium at 20 °C. After 20 min a slurry of **15** (2.61 g, 4.19 mmol) in *n*-hexane (20 mL) was added. After a period of 4 d of stirring at room temperature it was filtered. The filtrate was discarded and the filter-cake was continuously extracted with *n*-hexane for 7 d. During this time a colourless precipitate separated, which was crystallized form CH_2Cl_2/n-hexane to give product **16** (0.63 g, 53% yield) as a microcrystalline solid. ^{1}H-NMR ($CDCl_3$): δ = 1.77 (d, $^3J_{HH}$ = 6.3 Hz, 12H, CH(C*H*$_3$)$_2$), 4.56 (sept., $^3J_{HH}$ = 6.3 Hz, 2H, C*H*(CH$_3$)$_2$), 7.11 (m, 2H, CH-diazaborolyl), 7.19 (m, 2H, CH-diazaborolyl), 7.30-7.38 (m, 2H, CH-diazaborolyl and 6H, *m* -and *p*-CH-phenyl), 7.41 (m, 2H, CH-diazaborolyl), 7.53 (m, 4H, *o*-CH-phenyl), 7.72 (s, 4H, 1,4-phenylendiamine C=CH-CH=C) ppm. ^{13}C{^{1}H}-NMR ($CDCl_3$): δ = 23.4 (s, CH(*C*H$_3$)$_2$), 46.2 (s, *C*H(CH$_3$)$_2$), 107.3(s, B-C≡*C*), 109.8 (s, CH-diazaborolyl), 110.3 (s, CH-diazaborolyl), 119.3 (s, CH-diazaborolyl), 120.0 (s, CH-diazaborolyl), 123.1 (s, C≡C-*C*), 126.6 (s, 1,4-phenylendiamine C=*C*H-*C*H=C), 128.4 (s, *m*-CH-phenyl), 128.9 (s, *p*-CH-phenyl), 131.9 (s, *o*-CH-phenyl), 133.2 (s, 1,4-phenylendiamine *C*=CH-CH=*C*), 136.7, 137.9 (2s, C-diazaborolyl) ppm. The borolyl B-*C*≡C peak was not observed. ^{11}B{^{1}H}-NMR ($CDCl_3$): δ = 20.2 (s) ppm. $C_{40}H_{36}B_2N_2$(594.36): calcd. C 80.83, H 6.11, N 9.43; found C 80.19, H 6.10, N 9.23.

2-Cyclohexylamino-1-bromobenzene (17): A mixture of 2-bromoaniline (5.00 g, 29.07 mmol), cyclohexanone (8.56 g, 87.2 mmol) and *p*-toluene sulfonic acid in 80 mL of benzene was refluxed with a Dean-Stark trap attached for 24 h. Solvent and excess of cyclohexanone were removed at 60°C *in vacuo*. The resulting oil was dissolved in methanol (100 mL) and treated with $NaBH_4$ (3.4 g, 90.0 mmol) in an ice bath. The reaction mixture was stirred for 16 h during which the bath reached ambient temperature. An aqueous solution of sodium hydroxide (150 mL, 1 M) was added and the organic layer was removed. The aqueous layer was extracted with CH_2Cl_2 (3x100 mL) before the combined organic phases were dried with Na_2SO_4. It was filtered and the filtrate was evaporated to dryness. Remaining starting material was removed by filtration of a toluene solution over a pad (l = 15cm, Ø = 5cm) of silica 60. After washing with toluene the elute was freed from solvent. The subsequent short path distillation of the residue (10^{-6} bar, 90 °C bath temperature) furnished product **17** as colourless liquid (yield: 4.50 g, 61%). ^{1}H-NMR ($CDCl_3$): δ = 1.26 (m, 3H, C_6H_{11}), 1.39 (m, 2H, C_6H_{11}), 1.65 (m, 1H, C_6H_{11}), 1.77 (m, 2H, C_6H_{11}), 2.04 (m, 2H, C_6H_{11}), 3.30 (m, 1H,

NCH), 4.23 (s, 1H, NH), 6.51 (m, 1H, H-phenylene), 6.64 (m, 1H, H-phenylene), 7.14 (m, 1H, H-phenylene), 7.40 (m, 1H, H-phenylene) ppm.

***N,N'*-(Bis-2'-cyclohexylamino-phenyl)-*p*-phenylenediamine (18):** Sodium *tert*-butanolate (0.023 g, 0.29 mmol), 1,3-bis(2,6-diisopropylphenyl)imidazolium chloride (0.092 g, 0.22 mmol) and palladium acetate (0.024 g, 0.11 mmol) were dissolved with stirring in hot toluene (5 mL, 80 °C). This solution was added to a mixture of *p*-phenylenediamine (1.17 g, 10.8 mmol), 5.50 g (21.6 mmol) of **17** and sodium *tert*-butanolate (2.29 g, 23.8 mmol) in 200 mL of toluene. The solution was heated for 72 h at 110 °C, whereby solid NaBr precipitated. Then the dark solution was extracted with degassed saturated solutions of NH_4Cl (3x 50 mL) and NaCl (1x50 mL).The organic layer was dried with Na_2SO_4, filtered and freed from solvent *in vacuo* to afford a dark blue oil. Two-fold recrystallisation from *n*-hexane furnished 2.5 g (51% yield) of product **18** as colourless crystals. ^{1}H-NMR (C_6D_6): δ = 0.94 (m, 6H, C_6H_{11}), 1.07 (m, 4H, C_6H_{11}), 1.39 (m, 2H, C_6H_{11}), 1.52 (m, 4H, C_6H_{11}), 1.87 (m, 4H, C_6H_{11}), 3.11 (m, 2H, N-CH), 4.01 (s, 1H, NH), 4.55 (s, 1H, NH), 6.31 (s, 4H, 1,4-phenylendiamine C=CH-CH=C), 6.56 (m, 2H, H-1,2-phenylenediamine), 6.72 (m, 2H, H-1,2-phenylenediamine), 7.01 (m, 2H, H-1,2-phenylenediamine), 7.08 (m, 1H, H-1,2-phenylenediamine) ppm. ^{13}C{^{1}H}-NMR (C_6D_6): δ = 24.6 (s, CH_2), 25.5 (s, CH_2), 31.5 (s, CH_2), 51.4 (s, CH-C_6H_{11}), 111.5, 117.7 (2s, CH-1,2-phenylenediamine), 118.1 (s, 1,4-phenylendiamine C=*C*H-*C*H=C), 123.8, 124.7 (2s, CH-1,2-phenylenediamine), 130.6 (s, 1,4-phenylendiamine *C*=CH-CH=*C*), 138.5, 142.9 (2s, C-1,2-phenylenediamine) ppm.

1,4-Bis[(2'-bromo-3'-cyclohexyl-1',3',2'-benzodiazaborol-1'yl)] benzene (19): A slurry of CaH_2 (1.1 g, 16.4 mmol) in CH_2Cl_2 (30 mL) was simultaneously combined with two separate solutions of **18** (2.3 g, 5.1 mmol) and boron tribromide each in 30 mL of CH_2Cl_2. The slurry was stirred for 16 h at ambient temperature, filtered and the filtrate was evaporated to dryness. The residue was crystallized from toluene to afford 1.38 g (43%) of **19** as a colourless solid. ^{1}H-NMR (C_6D_6): δ = 1.07 (m, 2H, C_6H_{11}), 1.18 (m, 4H, C_6H_{11}), 1.51 (m, 2H, C_6H_{11}), 1.66 (m, 4H, C_6H_{11}), 1.83 (m, 4H, C_6H_{11}), 2.19 (m, 4H, C_6H_{11}), 3.97 (m, 2H, NCH), 6.95 (m, 2H, CH-diazaborolyl), 7.05 (m, 2H, CH-diazaborolyl), 7.07 (m, 2H, CH-diazaborolyl), 7.22 (m, 2H, CH-diazaborolyl), 7.14 (s, 4H, 1,4-phenylendiamine C=CH-CH=C) ppm. ^{13}C{^{1}H}-NMR (C_6D_6): δ = 25.4, 26.3, 32.2 (3s, CH_2), 54.9 (s, CH-C_6H_{11}), 110.6, 110.7, 119.8, 120.3 (4s, CH-diazaborolyl), 128.1 (s, 1,4-phenylendiamine C=*C*H-*C*H=C), 135.7 (s, 1,4-phenylendiamine *C*=CH-CH=*C*), 137.4, 137.5 (2s, C-1,2-phenylenediamine) ppm. The borolyl B-*C*≡C peak was not observed. ^{11}B{^{1}H}-NMR (C_6D_6): δ = 23.5 (s) ppm. $C_{30}H_{34}BBr_2N_4$ (632.05): calcd. C 57.01, H 5.42, N 8.86; found: C 56.15, H 5.17, N 8.24.

1,4-Bis[2'-*p*-dimesitylboryl-phenylethynyl-3'-cyclohexyl-1',3',2'-benzodiazaborol-1-yl)]benzene (20): A toluene solution (40 mL) of 4-dimesitylboryl-phenylacetylene (1. 05 g, 3.0 mmol) was treated at 20 °C with 1.88 mL of a 1.6 M *n*-hexane solution (20 mL) of *n*-butyllithium (3.0 mmol).After 20 min a toluene solution (20 mL) of compound **19** (0.95 g, 1.5 mmol) was added at 20 °C and stirring was continued for 16 h. Solvent and volatile components were removed *in vacuo* and the residue was stirred in 60 mL of *n*-hexane. After filtration the filtrate was discarded and the filter-cake was continuously extracted with *n*-

hexane over a period of 14 d. Thereby a colourless precipitate separated, which was collected by filtration and subsequently recrystallised from a toluene/*n*-hexane mixture. Product **20** was obtained as a colourless microcrystalline solid (0.21 g, 12% yield). ^{1}H-NMR (C_6D_6): δ= 1.23 (m, 6H, C_6H_{11}), 1.61 (m, 2H, C_6H_{11}), 1.73 (m, 4H, C_6H_{11}), 2.05 (s, 12H, *o*-CH_3- mesityl), 2.08 (m, 4H, C_6H_{11}), 2.18 (s, 6H, *p*-CH_3- mesityl), 2.29 (m, 4H, C_6H_{11}), 3.91 (m, 2H, NCH), 6.76 (s, 4H, CH-mesityl), 6.99 (m, 2H, CH-diazaborolyl), 7.05 (m, 2H, CH-diazaborolyl), 7.19 (m, 2H, CH-diazaborolyl), 7.31 (m, 2H, CH-diazaborolyl), 7.43 (d, $^{3}J_{HH}$ = 8.4 Hz, 1,4-phenylene), 7.48 (d, $^{3}J_{HH}$ = 8.4 Hz, 1,4-phenylene), 7.56 (s, 4H, 1,4-phenylendiamine C=CH-CH=C) ppm. ^{13}C{^{1}H}-NMR (C_6D_6): δ = 21.0 (s, *p*-CH_3-mesityl), 23.5 (s, *o*-CH_3- mesityl), 25.6, 26.9, 32.5 (3s, CH_2), 54.2 (s, CH-C_6H_{11}), 107.3 (s, B-C≡*C*), 109.7, 110.2, 119.1, 119.8 (4s, CH-diazaborolyl), 126.2 (s, C≡C-*C*), 126.4 (s, 1,4-phenylendiamine C=*C*H-*C*H=C), 128.7 (s, CH-mesityl), 131.2 (s, CH-1,4-phenylene), 133.1 (s, 1,4-phenylendiamine *C*=CH-CH=*C*), 136.0 (s, CH-1,4-phenylene), 136.6, 137.8 (2s, C-diazaborolyl), 138.9 (s, *p*-C-mesityl), 140.6 (s, *o*-C- mesityl), 141.5 (s, BC- mesityl), 146.5 (s, BC-1,4-phenylene) ppm. The borolyl B-*C*≡C peak was not observed. ^{11}B{^{1}H}NMR (C_6D_6): δ = 21.0 (s, BN_2), 74.9 (s, $BMes_2$) ppm. $C_{82}H_{86}B_4N_4$(1170.8) calcd. C 84.12, H 7.40, N 4.79; found C 83.69, H 7.25, N 4.31.

X-ray Crystallography

Crystallographic data of compounds **3** and **12** were collected with a Bruker Nonius KappaCCD diffractometer with $Mo_{K\alpha}$ (graphite monochromator, λ = 0.71073 Å) at 100 K (12 at 200 K), while **[Bu$_4$N][12·F]** and **15** were measured on a Bruker AXS X8 with $Cu_{K\alpha}$ radiation at 100 K. Crystallographic programs used for structure solution and refinement were SHELXS-97 and SHELXL-97.[39] The structures were solved by direct methods and were refined by using full-matrix least squares of $\underline{F}^2$ of all unique reflections with anisotropic thermal parameters for all non-hydrogen atoms. Hydrogens atoms were included at calculated positions with U(H) = 1.2 U_{eq} for CH_2 groups and U(H) = 1.5U_{eq} for CH_3 groups. Crystallographic data for the compounds are listed in Table 6.

Table **6**: Crystallographic data of **3**, **12**, **[Bu$_4$N][12·F]** and **15**.

	3	**12**	**[Bu$_4$N][12·F]**	**15**
Empirical formula	$C_{36}H_{40}B_2N_2$	$C_{34}H_{38}B_2N_2S$	$C_{50}H_{74}B_2FN_3S$	$C_{24}H_{26}B_2Br_2N_4$
*M*r [g mol^{-1}]	522.32	528.34	789.80	551.93
Crystal dimension (mm)	0.30x0.30x0.04	0.21x0.06x0.04	0.31x0.16x0.08	0.33x0.21x0.16
Crystal system	monoclinic	triclinic	triclinic	monoclinic
Space group	$P2_1$	$P\bar{1}$	$P\bar{1}$	$P2_1/c$
a[Å]	8.4437(2)	8.1825(4)	18.230(3)	9.1033(5)
b [Å]	9.4089(2)	13.9608(5)	22.799(4)	7.6616(4)
c [Å]	19.3916(4)	14.0110(7)	24.997(4)	17.2575(9)
α [°]	90	82.544(3)	106.930(11)	90
β [°]	97.7092(11)	83.797(2)	99.728(14)	90.917(2)
γ [°]	90	74.747(2)	94.965(11)	90
V [Å]	1526.66(6)	1526.52(12)	9694(3)	1203.48(11)
Z	2	2	8	2

ς_{calc} [g cm^{-3}]	1.136	1.149	1.082	1.523
μ [mm^{-1}]	0.064	0.131	0.876	4.412
F (000)	560	564	3440	556
Θ [ºC]	3.0-27.5	2.9-25.0	1.9-66.4	4.9-72.0
No refl. collected	32337	16943	53217	20670
No refl. unique	3700	5359	30945	2343
R (int)	0.052	0.046	0.0250	0.0439
No refl. [I→2σ(I)]	3303	3741	25380	2342
Refined parameters	369	360	2101	148
GOF	1.024	1.017	1.017	1.083
R_f [I→2σ(I)]	0.0364	0.0488	0.0494	0.0500
wR_F2 (all data)	0.0879	0.1340	0.1406	0.1184
$\Delta\varsigma_{max/min}$ [eÅ^{-3}]	0.188/-0.165	0.204/-0.227	0.904/-0.291	2.729/-1.804
Remarks				Largest diff. Peak near Br(1)(0.77Å)

Computational methods

All computations were carried out with the Gaussian 03 and Gaussian 09 packages.[40] Geometries were optimized by DFT calculations at the B3LYP/6-31G* level of theory.[41,42] TD-DFT-calculations with the CAM-B3LYP[43] functional were performed on the B3LYP optimized geometries. Frequency calculations on the fully optimized geometries showed no imaginary frequencies. MO figures were generated with Molekel[44] and the GaussSum 2.2 package was used to calculate the orbital contributions.[45]

References

[1] a) C. D. Entwistle, T. B. Marder, Angew. Chem. **2002**, *114*, 3051–3056; *Angew. Chem. Int. Ed*. **2002**, *41*, 2927–2931; b) C. D. Entwistle, T. B. Marder, *Chem. Mater*. **2004**, *16*, 4574–4585; c) S. Yamaguchi, A. Wakamiya, *Pure Appl. Chem*. **2006**, *78*, 1413–1424; d) F. Jäkle, *Coord. Chem. Rev*. **2006**, *250*, 1107–1121.

[2] a) Z. Yuan, N.J. Taylor, T.B. Marder, I.D. Williams, S.K. Kurtz, L.-T. Cheng, *J. Chem. Soc., Chem. Commun*. **1990**, 1489-1492; b) Z. Yuan, N.J. Taylor, T.B. Marder, I.D. Williams, S.K. Kurtz, L.-T. Cheng, *Organic Materials for Non-linear Optic II* Ed. R.A. Hann, D. Bloor, RCS, Cambridge, **1991**, p.190; c) M. Lequan, R.M. Lequan, K. Chane-Ching, *J. Mater. Chem*. **1991**, *1*, 997-999; d) M. Lequan, R.M. Lequan, K. Chane-Ching, M. Barzoukas, A. Fort, H. Lahoucine, G. Bravic, J. Chasseau, J. Gaultier, *J. Mater. Chem*. **1992**, *2*, 719-725 ; e) M. Lequan, R.M. Lequan, K. Chane-Ching, A.-C. Callier, M. Barzoukas, A. Fort, *Adv. Mater. Opt. Electron*. **1992**, *1*, 243-247 ; f) Z. Yuan, N.J. Taylor, Y. Sun, T.B. Marder, I.D. Williams, L.-T. Cheng, *J. Organomet. Chem.* **1993**, *449*, 27-37; g) C. Branger, M. Lequan, R.M. Lequan, M. Barzoukas, A. Fort, *J. Mater. Chem*. **1996**, *6*, 555-558; h) Z. Yuan, N.J. Taylor, R. Ramachandran, T.B. Marder, *Appl. Organomet. Chem*. **1996**, *10*, 305-316; i) Z. Yuan, J.C. Collings, N.J. Taylor, T.B. Marder, C. Jardin, J.-F. Halet, *J. Solid State Chem.* **2000**, *154*, 5-12; j)

Y. Liu, X. Xu, F. Zheng, Y. Cui, *Angew. Chem.* **2008**, 120, 4614-4617; *Angew. Chem. Int. Ed.* **2008**, *47*, 4538-4541.

[3] Z. Yuan, C.D. Entwistle, J.C. Collings, D. Albesa-Jove, A.S. Batsanov, J.A.K. Howard, H.M. Kaiser, D.E. Kaufmann, S.-Y. Poon, W.-Y. Wong, C. Jardin, S. Fatallah, A. Boucekkine, J.-F. Halet, T.B. Marder, *Chem. Eur. J.* **2006**, *12*, 2758-2771.

[4] a) Z.-Q. Liu, Q. Fang, D. Wang, G. Xue, W.-T. Yu, Z.-S. Shao, M.-H. Jiang, *Chem. Commun*. **2002**, 2900-2901; b) Z.-Q. Liu, Q. Fang, D. Wang, D.-X. Cao, G. Xue, W.-T. Yu, H. Lei, *Chem. Eur. J*. **2003**, *9*, 5074-5084; c) D.-X. Cao, Z.-Q. Liu, Q. Fang, G.-B. Xu, G. Xue, G.-Q. Liu, W.-T. Yu, *J. Organomet. Chem*. **2004**, *689*, 2201-2206; d) Z.-Q. Liu, Q. Fang, D.-X. Cao, D. Wang, G.-B. Xu, *Org. Lett*. **2004**, *6*, 2933-2936; e) Z.-Q. Liu, M. Shi, F.-Y. Li, Q. Fang, Z.-H. Clen, T. Yi, C.-H. Huang, *Org. Lett*. **2005**, *7*, 5481-5484; f) M. Charlot, L. Porrès, C.D. Entwistle, A. Beeby, T.B. Marder, M. Blanchard-Desce, *Phys. Chem. Chem. Phys*. **2005**, *7*, 600-606; g) L. Porrès, M. Charlot, C.D. Entwistle, A. Beeby, T.B. Marder, M. Blanchard-Desce, *Proc. SPIE-Int. Soc. Opt. Engl*. **2005**, *5934*, 92; h) D-X. Cao, Z-Q. Liu, G-Z. Li, G.-Q. Liu, G.-H. Zhang, *J. Mol. Struct*. **2008**, *874*, 46-50; i) J.C. Collings, S-Y. Poon, G. Le Droumarguet, M. Charlot, C. Katan, L-O. Palsson, A. Beeby, J.A. Mosely, H.M. Kaiser, D. Kaufmann, W-Y. Wong, M. Blanchard-Desce, T.B. Marder, *Chem. Eur. J*. **2009**, *15*, 198-208; j) S.-B. Zhao, P. Wucher, Z. M. Hudson, T. M. McCormick, X.-Y. Liu, S. Wang, X.-D. Feng, Z.-H. Lu *Organometallics* **2008**, *27,* 6446–6456.

[5] a) T. Noda, Y. Shirota, *J. Am. Chem. Soc*. **1998**, *120*, 9714-9715; b) T. Noda, H. Ogawa, Y. Shirota*, Adv. Mater*. **1999**, *11*, 283-285; c) T. Noda, Y. Shirota, *J. Lumin*. **2000**, *87-89*, 1168-1170; d) Y. Shirota, M. Kinoshita, T. Noda, K. Okumuto, T.Ohara, *J. Am. Chem. Soc*. **2000**, *122*, 11021-11022; e) M. Kinoshita, N. Fujii, T. Tsukaki, Y. Shirota, *Synth.Met.* **2001**, *121*, 1571-1572; f) H. Doi, M. Kinoshita, K. Okumoto, Y. Shirota, *Chem. Mater*, **2003**, *15*, 1080-1089; g) W.-L. Jia, D.-R. Bai, T.Mc Cormick, Q-D. Liu, M. Motala, R-Y. Wang, C. Seward, Y. Tao, S. Wang, *Chem. Eur. J.* **2004**, *10*, 994-1006; h) W-L. Jia, D. Feng, D-R. Bai, Z.H. Lu, S. Wang, G. Vamvounis, *Chem. Mater*. **2005**, *17*, 164-170; i) W-L. Jia, M.J. Moran, Y-Y. Yuan, Z.H. Lu, S. Wang, *J. Mater. Chem*. **2005**, *1*5, 3326-3333; j) M. Mazzeo, V. Vitale, F. Della Sala, M. Anni, G. Barbarella, L. Favaretto, G. Sotgui, R. Cingolani, G.Gigli, *Adv. Mater*. **2005**, *17*, 34-39; k) G.-J. Zhou, G.-L. Ho, W.-Y. Wong, Q. Wang, D.-G. Ma, L.-X. Wang, Z.-Y. Lin, T.B. Marder, A. Beeby, *Adv. Funct. Mater*. **2008**, *18*, 499-511.

[6] M. E. Glogowski, J. L. R. Williams, *J. Organomet. Chem.* **1981**, *218*, 137-146.

[7] A. Schulz, W. Kaim, *Chem. Ber.* **1989**, *122*, 1863-1868.

[8] J. C. Doty, B. Babb, P. J. Grisdale, M. E. Glogowski, J. L. R. Williams, *J. Organomet. Chem.* **1972**, *38*, 229-236.

[9] a) S. Yamaguchi, S. Akiyama, K. Tamao, *J. Am. Chem. Soc.* **2001**, *123*, 11372-11375; b) S. Yamaguchi, T. Shirasaka, S. Akiyama, K. Tamao, *J. Am. Chem. Soc.* **2002**, *124*, 8816-8817; c) Y. Kubo, M. Yamamoto, M. Ikeda, M. Takeuchi, S. Shinkai, S. Yamaguchi, K. Tamao, *Angew. Chem.* **2003**, *115*, 2082-2086; *Angew. Chem. Int. Ed.* **2003**, *42*, 2036-2040.

[10] a) S. Solé, F. P. Gabbaï, *Chem. Commun.* **2004**, 1284-1285; b) M. Melaïmi, F. P. Gabbaï, *J. Am. Chem. Soc.* **2005**, *127*, 9680-9681; c) T. W. Hudnall, M. Melaïmi, F. P.

Gabbaï, *Org. Lett.* **2006**, *8*, 2747-2749; d) C.-W. Chiu, F. P. Gabbaï, *J. Am. Chem. Soc.* **2006**, *128*, 14248-14249; e) M. H. Lee, T. Agou, J. Kobayashi, T. Kawashima, F. P. Gabbaï, *Chem. Commun.* **2007**, 1133-1135; f) T. W. Hudnall, F. P. Gabbaï, *J. Am. Chem. Soc*. **2007**, *129*, 11978-11986; g) Y. Kim, F. P. Gabbaï, *J. Am. Chem. Soc.* **2009**, *131*, 3363-3369.

[11] a) A. Sundararaman, M. Victor, R. Varughese, F. Jäkle, *J. Am. Chem. Soc.* **2005**, *127*, 13748-13749; b) K. Parab, K. Venkatasubbaiah, F. Jäkle, *J. Am. Chem. Soc.* **2006**, 128, 12879-12885.

[12] a) E. Sakuda, A. Funahashi, N. Kitamura, *Inorg. Chem.* **2006**, *45*, 10670-10677; b) M.-S. Yuan, Z.-Q. Liu, Q. Fang, *J. Org. Chem.* **2007**, *72*, 7915-7922.

[13] a) D.-R. Bai, X.-Y. Liu, S. Wang, *Chem. Eur. J.* **2007**, *13*, 5713-5723; b) S.-B. Zhao, T. McCormick, S. Wang, *Inorg. Chem.* **2007**, *46*, 10965-10967; c) X. -Y. Liu, D. -R. Bai, S. Wang, *Angew. Chem.* **2006**; *Angew. Chem. Int. Ed.* **2006**, *45*, 5475-5478.

[14] a) L. Weber, *Coord. Chem. Rev.* **2001**, *215,* 39-77; b) L.Weber, *Coord. Chem. Rev*. **2008**, *252*, 1-31.

[15] a) M. Yamashita, K. Nozaki, *J. Synth. Org. Chem*. **2010**, *68*, 359-369; b) M. Yamashita, K. Nozaki, *Pure Appl. Chem.* **2008**, *80*, 1187-1194; c) M. Yamashita, K. Nozaki, *Bull. Chem. Soc. Jpn.* **2008**, *81*, 1377-1392.

[16] L. Weber, H. B. Wartig, H.-G. Stammler, B. Neumann, *Organometallics* **2001**, *20*, 5248-5250.

[17] L. Weber, H. B. Wartig, H.-G. Stammler, B. Neumann, *Z. Anorg. Allg. Chem.* **2001**, *627*, 2663-2668.

[18] L. Weber, I. Domke, W. Greschner, K. Miqueu, A. Chrostowska, P. Baylère, *Organometallics* **2005**, *24*, 5455-5463.

[19] For examples of recent work on 1,3,2-diazaboroles, see a) T. Habereder, H. Nöth, *Appl. Organomet. Chem*. **2003**, *17*, 525-538; b) L. Weber, I. Domke, J. Kahlert, H.-G. Stammler, *Eur. J. Inorg. Chem.* **2006**, 3419-3424; c) L. Weber, A. Rausch, H.-G. Stammler, B. Neumann, *Z. Anorg. Allg. Chem.* **2004**, *630*, 2657-2664; d) L. Weber, J. Förster, H.-G. Stammler, B. Neumann, *Eur. J. Inorg. Chem.* **2006**, 5048-5056; L. Weber, M. Schnieder, T. C. Maciel, H. B. Wartig, M. Schimmel, R. Boese, D. Bläser, *Organometallics* **2000**, *19*, 5791-5794; e) J. M. Murphy, J. D. Lawrence, K. Kawamura, C. Incarvito, J. F. Hartwig, *J. Am. Chem. Soc.* **2006**, *128*, 13684**-**13685; f) Y. Segawa, M. Yamashita, K. Nozaki, *Science* **2006**, *314*, 113-115; g) T.B. Marder, *Science* **2006**, *314*, 69-70; h) H. Braunschweig, *Angew. Chem.* **2007**, *119*, 1990-1992; *Angew. Chem. Int. Ed.* **2007**, *46*, 1946-1948; i) Y. Segawa, M. Yamashita, K. Nozaki, *Angew. Chem.* **2007**, *119*, 6830-6833; *Angew. Chem. Int. Ed.* **2007**, *46*, 6710-6713; j) T. Kajiwara, T. Terabayashi, M. Yamashita, K. Nozaki, *Angew. Chem.* **2008**, *120*, 6708-6712; *Angew. Chem. Int. Ed.* **2008**, *47*, 6606-6610; k) Y. Segawa, Y. Suzuki, M. Yamashita, K. Nozaki, *J. Am. Chem. Soc.* **2008**, *130*, 16069-16079; l) M. Yamashita, Y. Suzuki, Y. Segawa, K. Nozaki, *Chem. Lett.* **2008**, *37*, 802-803; m) T. Terabayashi, T. Kajiwara, M. Yamashita, K. Nozaki, *J. Am. Chem. Soc.* **2009**, *131*, 14162-14163; n) A. Hinchcliffe, F. S. Mair, E. J. L. Mc Innes, R. G. Pritchard, J. E. Warren, *Dalton Trans.* **2008**, 222-233; o) E. Giziroglu, B. Donnadieu, G. Bertrand, *Inorg. Chem*. **2008**, *47*, 9751-9753; p) L. Weber, V. Werner, M.A. Fox, T. B. Marder, S. Schwedler, A. Brockhinke, H.-G.

Stammler, B. Neumann, *Dalton Trans*. **2009**, 1339-1351; q) L. Weber, J. Halama, V. Werner, K. Hanke, L. Böhling, A. Chrostowska, A. Dargelos, M. Maciejczyk, A.-L. Raza, H.-G. Stammler, B. Neumann *Eur. J. Inorg. Chem*. **2010**, 5416-5425.

[20] S. Maruyama, Y. Kawanishi, *J. Mater. Chem*. **2002**, *12*, 2245-2249.

[21] L. Weber, I. Domke, C. Schmidt, T. Braun, H.–G. Stammler, B. Neumann, *Dalton Trans.* **2006**, 2127-2132.

[22] L.Weber, A. Penner, I. Domke, H.-G. Stammler, B. Neumann, *Z. Anorg. Allg. Chem*. **2007**, *633*, 563-569.

[23] L. Weber, D. Eickhoff, V. Werner, L. Böhling, S. Schwedler, A. Chrostowska, A. Dargelos, M. Maciejczyk, H.–G. Stammler, B. Neumann, *Dalton Trans.* **2011**, *40*, 4434-4446.

[24] S. Schwedler, D. Eickhoff, R. Brockhinke, D. Cherian, L. Weber, A. Brockhinke, *Phys. Chem. Chem. Phys.* **2011**, *13*, 9301-9310.

[25] L. Weber, V. Werner, I. Domke, H.-G. Stammler, B. Neumann, *Dalton Trans.* **2006**, 3777-3784.

[26] A. Chrostowska, M. Maciejczyk, A. Dargelos, P. Baylère, L. Weber, V. Werner, D. Eickhoff, H.-G. Stammler, B. Neumann, *Organometallics* **2010**, *29*, 5192-5198.

[27] L. Weber, V. Werner, M. A. Fox, T. B. Marder, S. Schwedler, A. Brockhinke, H.-G. Stammler, B. Neumann, *Dalton Trans*. **2009**, 2823-2831.

[28] L. Weber, D. Eickhoff, T. B. Marder, M. A. Fox, P. J. Low, A. D. Dwyer, D. J. Tozer, S. Schwedler, A. Brockhinke, H.-G. Stammler, B. Neumann, *Chem. Eur. J*. **2012**, *18*, 1369-1382.

[29] J.A. Marsden, J.J. Miller, L.D. Shirtcliff, M.M. Haley, *J. Am. Chem. Soc.* **2005**, *127*, 2464-2476.

[30] Z. An, S. A. Odom, R. F. Kelley, C. Huang, X. Zhang, S. Barlow, L. A. Padilha, J. Fu, S. Webster, D. J. Hagan, E. W. Van Stryland, M. R. Wasielewski, S. R. Marder, *J. Phys. Chem. A* **2009**, *119*, 5585-5593.

[31] S. P. Mc Ilroy, E. Cló, L. Nikolajsen, P. K. Frederiksen, C. B. Nielsen, K. V. Mikkelsen, K. V. Gothelf, P. R. Ogilby, *J. Org. Chem.* **2005**, *70*, 1134-1146.

[32] E. C.-H. Kwok, M.-Y. Chan, K. M.-C. Wong, W. H. Lam, V. W.-W. Yam, *Chem. Eur. J*, **2010**, *16*, 12244-12254.

[33] A. Pelter, K. Smith, H. C. Brown, *Borane Reagents*, Academic Press London, **1988**, p.428.

[34] L. Jafarpour, E. D. Stevens, S. P. Nolan, *J. Organomet. Chem.* **2000**, *606*, 49-54.

[35] G. Zhou, M. Baumgarten, K. Müllen, *J. Am. Chem. Soc.* **2008**, *130*, 12477-12484.

[36] A. Dreuw, J. L. Weisman, M. Head-Gordon, *J. Chem. Phys.* **2003**, *119*, 2943-2946.

[37] M. J. G. Peach, P. Benfield, T. Helgaker, D. J. Tozer, *J. Chem. Phys.* **2008**, *128*, 044118.

[38] B. J. Lynch, P. L. Fast, M. Harris, D. G. Truhlar, *J. Phys. Chem. A*, **2000**, *104*, 4811-4815.

[39] "A short history of SHELX". G.M. Sheldrick, *Acta Cryst*. **2008**, *A64*, 112-122.

[40] a) Gaussian 03, Revision E.01, M. J. Frisch, G. W. Trucks, H. B. Schlegel, G. E. Scuseria, M. A. Robb, J. R. Cheeseman, J. A. Montgomery, Jr., T. Vreven, K. N. Kudin, J. C. Burant, J.M. Millam, S. S. Iyengar, J. Tomasi, V. Barone, B. Mennucci, M. Cossi, G. Scalmani, N. Rega, G. A. Petersson, H. Nakatsuji, M. Hada, M. Ehara, K. Toyota, R.

Fukuda, J. Hasegawa, M. Ishida, T. Nakajima, Y. Honda, O. Kitao, H. Nakai, M. Klene, X. Li, J. E. Knox, H. P. Hratchian, J. B. Cross, V. Bakken, C. Adamo, J. Jaramillo, R. Gomperts, R. E. Stratmann, O. Yazyev, A. J. Austin, R. Cammi, C. Pomelli, J. W. Ochterski, P. Y. Ayala, K. Morokuma, G. A. Voth, P. Salvador, J. J. Dannenberg, V. G. Zakrzewski, S. Dapprich, A. D. Daniels, M. C. Strain, O. Farkas, D. K. Malick, A. D. Rabuck, K. Raghavachari, J. B. Foresman, J. V. Ortiz, Q. Cui, A. G. Baboul, S. Clifford, J. Cioslowski, B. B. Stefanov, G. Liu, A. Liashenko, P. Piskorz, I. Komaromi, R. L. Martin, D. J. Fox, T. Keith, M. A. Al-Laham, C. Y. Peng, A. Nanayakkara, M. Challacombe, P. M. W. Gill, B. Johnson, W. Chen, M. W. Wong, C. Gonzalez, and J. A. Pople, *Gaussian, Inc.*, Wallingford CT **2004**; b) Gaussian 09, Revision A.02, M. J. Frisch, G. W. Trucks, H. B. Schlegel, G. E. Scuseria, M. A. Robb, J. R. Cheeseman, G. Scalmani, V. Barone, B. Mennucci, G. A. Petersson, H. Nakatsuji, M. Caricato, X. Li, H. P. Hratchian, A. F. Izmaylov, J. Bloino, G. Zheng, J. L. Sonnenberg, M. Hada, M. Ehara, K. Toyota, R. Fukuda, J. Hasegawa, M. Ishida, T. Nakajima, Y. Honda, O. Kitao, H. Nakai, T. Vreven, J. J. A. Montgomery, J. E. Peralta, F. Ogliaro, M. Bearpark, J. J. Heyd, E. Brothers, K. N. Kudin, V. N. Staroverov, R. Kobayashi, J. Norm, K. Raghavachari, A. Rendell, J. C. Burant, S. S. Iyengar, J. Tomasi, M. Cossi, N. Rega, J. M. Millam, M. Klene, J. E. Knox, J. B. Cross, V. Bakken, C. Adamo, J. Jaramillo, R. Gomperts, R. E. Stratmann, O. Yazyev, A. J. Austin, R. Cammi, C. Pomelli, J. W. Ochterski, R. L. Martin, K. Morokuma, V. G. Zakrzewski, G. A. Voth, P. Salvador, J. J. Dannenberg, S. Dapprich, A. D. Daniels, O. Farkas, J. B. Foresman, J. V. Ortiz, J. Cioslowski, D. J. Fox, *Gaussian, Inc.*, Wallingford CT **2009**.

[41] a) A. D. Becke, *J. Chem. Phys.* **1993**, *98*, 5648-5652; b) C. Lee, W. Yang, G. Parr, *Phys. Rev. B: Condens. Matter Mater. Phys.* **1988**, *37*, 785-789.

[42] a) G. A. Petersson, M. A. Al-Laham, *J. Chem. Phys.* **1991**, *94*, 6081–6090; b) G. A. Petersson, A. Bennett, T. G. Tensfeldt, M. A. Al-Laham, W. A. Shirley, J. Mantzaris, *J. Chem. Phys.* **1988**, *89*, 2193–2218.

[43] T. Yanai, D. P. Tew, N. C. Handy, *Chem. Phys. Lett.* **2004**, *393*, 51-57.

[44] U. Varetto, *MOLEKEL Version*, Swiss National Supercomputing Centre, Mann, Switzerland.

[45] N. M. O'Boyle, A. L. Tenderholt, K. M. Langner, *J. Comp. Chem.* **2008**, *29*, 839-845.